Tectonics®

RESEARCH ARTICLE

Key Points:

- The Le May Group forms part of the extensive Permian accretionary complexes of West Gondwana and has a depositional age of c. 255 Ma
- Accretion developed during the mid-Triassic, potentially related to the Peninsula Orogeny and an episode of flat-slab subduction
- A para-autochthonous origin is suggested for the youngest unit, with Cretaceous accretion associated with mélange belts of oceanic material

Correspondence to:

T. R. Riley,
trr@bas.ac.uk

Evolution of an Accretionary Complex (LeMay Group) and Terrane Translation in the Antarctic Peninsula

Teal R. Riley[1] , **Ian L. Millar[2]** , **Andrew Carter[3]** , **Michael J. Flowerdew[4]**, **Alex Burton-Johnson[1]** , **Joaquin Bastias[5,6]** , **Craig D. Storey[7]** , **Paula Castillo[8]**, **David Chew[5]** , and **Martin J. Whitehouse[9]**

[1]British Antarctic Survey, Cambridge, UK, [2]British Geological Survey, Nottingham, UK, [3]Department of Earth and Planetary Sciences, Birkbeck, University of London, London, UK, [4]CASP, Madingley Rise, Cambridge, UK, [5]Department of Geology, Trinity College Dublin, Dublin, Ireland, [6]Escuela de Geología, Facultad de Ingeniería, Universidad Santo Tomás, Santiago, Chile, [7]School of the Environment, Geography and Geosciences, University of Portsmouth, Portsmouth, UK, [8]Institut für Geologie und Paläontologie, Westfälische Wilhelms-Universität, Münster, Germany, [9]Swedish Museum of Natural History, Stockholm, Sweden

Abstract The LeMay Group accretionary complex of Alexander Island (Antarctic Peninsula) comprises a 4 km thick succession of variably deformed turbidites associated with thrust slices of ocean floor basalts. The depositional age and provenance of the succession is uncertain with estimates ranging from Carboniferous to Cretaceous. The accretion history is also poorly established and whether the LeMay Group developed allochthonously and accreted during an episode of Cretaceous terrane translation. We have examined the geochronology and geochemistry of 22 samples from across the entire accretionary complex to determine its depositional, provenance and accretion history. The accretionary complex has been subdivided into four separate groups based on detrital zircon U-Pb age and Lu-Hf provenance analysis. Groups 1 and 2 are interpreted to be a continuation of the extensive Permian accretionary complexes of West Gondwana and have a depositional age of c. 255 Ma, with volcaniclastic input from the extensive silicic volcanism of the Choiyoi Province. Accretion of the LeMay Group to the continental margin developed during the mid-Triassic, potentially related to the Peninsula Orogeny and an episode of flat-slab subduction of the proto-Pacific plate. Group 3 is only identified from an island to the west of Alexander Island and has a mid-Cretaceous depositional age and provenance akin to offshore sequences from Thurston Island. A para-autochthonous origin is suggested, with mid-Cretaceous accretion associated with the melange belts of central Alexander Island. Group 4 is also a distinct unit with an Early Jurassic depositional age and a source more closely related to the Antarctic Peninsula.

1. Introduction

From the Permian to the Cenozoic, the Antarctic Peninsula was the site of a long-lived convergent margin that led to widespread magmatism, the development of accretionary complexes, and thick fore-arc and back-arc sedimentary successions (Burton-Johnson & Riley, 2015; Figure 1). Alexander Island, situated to the west of the Antarctic Peninsula (Figure 2), is comprised of an extensive subduction-accretion complex, which is in structural contact with a fore-arc succession. The accretionary complex is termed the LeMay Group (Edwards, 1980) and incorporates variably deformed trench-fill turbidites and components of ocean floor and ocean island lithologies. Its age, provenance, accretion and paleo-location is poorly constrained, although a general younging toward the subducting margin (east to west) is suggested from field investigations (Tranter, 1988). In this study, 21 samples from 10 sites across the entire LeMay Group have been selected for combined detrital zircon (U-Pb and Lu-Hf) and white mica (^{40}Ar/^{39}Ar) analyses to understand the provenance of the accretionary complex and the role of accreted terranes as part of the tectonic history of the Antarctic Peninsula during the Mesozoic.

2. Antarctic Peninsula: Geological Setting

2.1. Background Geology

The Antarctic Peninsula is an arcuate mountainous belt that reaches heights of 3,200 m (Figure 2) and preserves a complex geological and tectonic history from the Ordovician to the present day; its geological record has been shaped by subduction along the proto-Pacific margin of West Gondwana and rifting in the Weddell Sea (Dalziel et al., 2013; Jordan et al., 2020).

Writing – review & editing: Teal R. Riley

The geological history of the Antarctic Peninsula is largely defined by the magmatic, depositional and deformation events of the Late Paleozoic and Mesozoic. These events were initially interpreted as a consequence of subduction and the development of an accretionary continental arc on Paleozoic basement of the Gondwana margin (Suárez, 1976; Thomson & Pankhurst, 1983) and is interpreted to form a belt that extends along the entire Pacific margin as part of the Terra Australis Orogen (Cawood, 2005). There is broad consensus on the accretionary nature of the orogeny, but the role of terranes and their translation during the Mesozoic remains an area of debate. Vaughan and Storey (2000) reinterpreted the geology of the Antarctic Peninsula as an amalgamation of para-autochthonous and allochthonous terranes following the development of similar models elsewhere along the Pacific margin in New Zealand (e.g., Robertson et al., 2019). The model was further developed to describe the accretion of terranes onto the Gondwana margin (e.g., Vaughan et al., 2012). However, Burton-Johnson and Riley (2015) have challenged this tectonic model and preferred an in situ continental arc development for the Peninsula, which has been supported by recent paleomagnetic data from the northern Antarctic Peninsula (Gao et al., 2021) and analysis of Mesozoic magmatic rocks (Bastias et al., 2020, 2021).

2.2. Alexander Island

The terrane model of Vaughan and Storey (2000) identified Alexander Island as a separate, potentially exotic terrane, termed the Western Domain (Figure 1), which comprises four geological units (Figure 3): a subduction and accretion complex, the LeMay Group (the subject of this paper), unconformably overlain, or in faulted contact with, the relatively shallow water fore-arc basin sedimentary rocks of the Fossil Bluff Group. The Fossil Bluff Group forms one of the most complete fore-arc successions globally with a sedimentary record almost 8 km in thickness (Butterworth et al., 1988). The LeMay Group is cut by Cenozoic granites and locally overlain by Late Cretaceous to Cenozoic volcanic rocks (McCarron & Millar, 1997). Neogene alkaline volcanic rocks were emplaced after the cessation of subduction and form relatively widespread volcanic fields across western and northern Alexander Island (Figure 3), and form part of the more extensive Bellingshausen Sea volcanic field (Smellie & Hole, 2021).

2.3. LeMay Group Accretionary Complex

The LeMay Group is a thick (c. 4 km), variably deformed succession of trench-fill turbidites and trench-slope units, associated with ocean floor and ocean island igneous and sedimentary rocks (Tranter, 1991). The LeMay Group has been interpreted as an accretionary complex (Tranter, 1988), consistent with the development of high pressure-low temperature blueschist-facies metamorphic assemblages (e.g., Wendt et al., 2008) from central Alexander Island (northern Lully Foothills and southeast Colbert Mountains; Figure 2). It is thought to have developed in a continental margin setting along the proto-Pacific margin (Burton-Johnson & Riley, 2015) or as part of an allochthonous terrane (Vaughan et al., 2002). The LeMay Group has a polyphase structural history that can be interpreted in the context of an accretion-subduction complex. The earliest deformational event is recognised across the LeMay Group succession and is related to thrust faults in poorly lithified sediments. A later phase of westward-verging folds and westward-directed thrusts deformed this earlier structure and was related to strike-slip movement in the arc prism (Tranter, 1987). The LeMay Group has been correlated to the Miers Bluff Formation of Livingston Island (part of the South Shetland Islands—Figure 1; Hervé et al., 2006; Bastias et al., 2019), who also drew comparisons to the Trinity Peninsula Group metasedimentary rocks of northern Graham Land (Figure 1).

The age of the LeMay Group is poorly constrained; *Radiolaria* in chert horizons indicate a Late Jurassic—Cretaceous age (Holdsworth & Nell, 1992) for parts of the Group in northern and central Alexander Island (Debussy Heights and Atoll Nunataks; Figure 3). At two localities in the Lully Foothills (Figure 2) an accreted volcanic island sequence contains an Early Jurassic shelly fauna (204–195 Ma; Thomson & Tranter, 1988), whereas macrofauna from northern Alexander Island, near Mount King (Figure 2), have been assigned Carboniferous and Permian ages (Kelly et al., 2001), although there is uncertainty regarding the exact relationship of the Mount King sequences to the rest of the LeMay Group. Stratigraphically some units of the LeMay Group have been assigned a likely Triassic age based on their relationship to the Early Jurassic units of the lowermost Fossil Bluff Group (Doubleday et al., 1993). A broad pattern of younging to the northwest is interpreted from the stratigraphic relationships, with evidence of east to west flowing paleocurrents, and a conglomerate clast source to the east. The youngest sequences are anticipated to crop out in Charcot Island to the west of Alexander Island (Tranter, 1988; Figure 3).
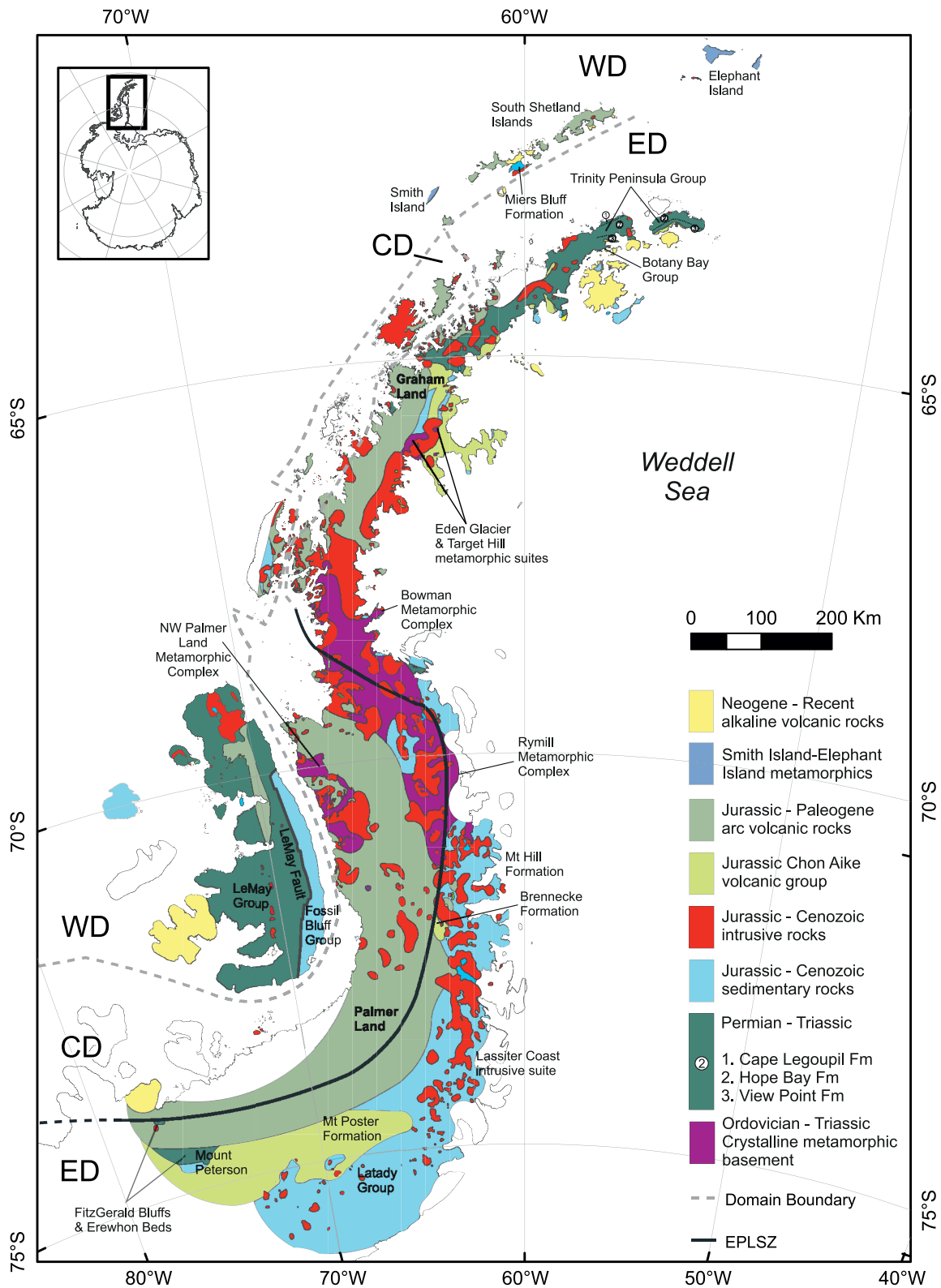
Figure 1. Geological map of the Antarctic Peninsula (after Burton-Johnson & Riley, 2015). PLSZ: Palmer Land shear zone; WD: Western domain; CD: Central Domain; ED: Eastern Domain (Vaughan & Storey, 2000).
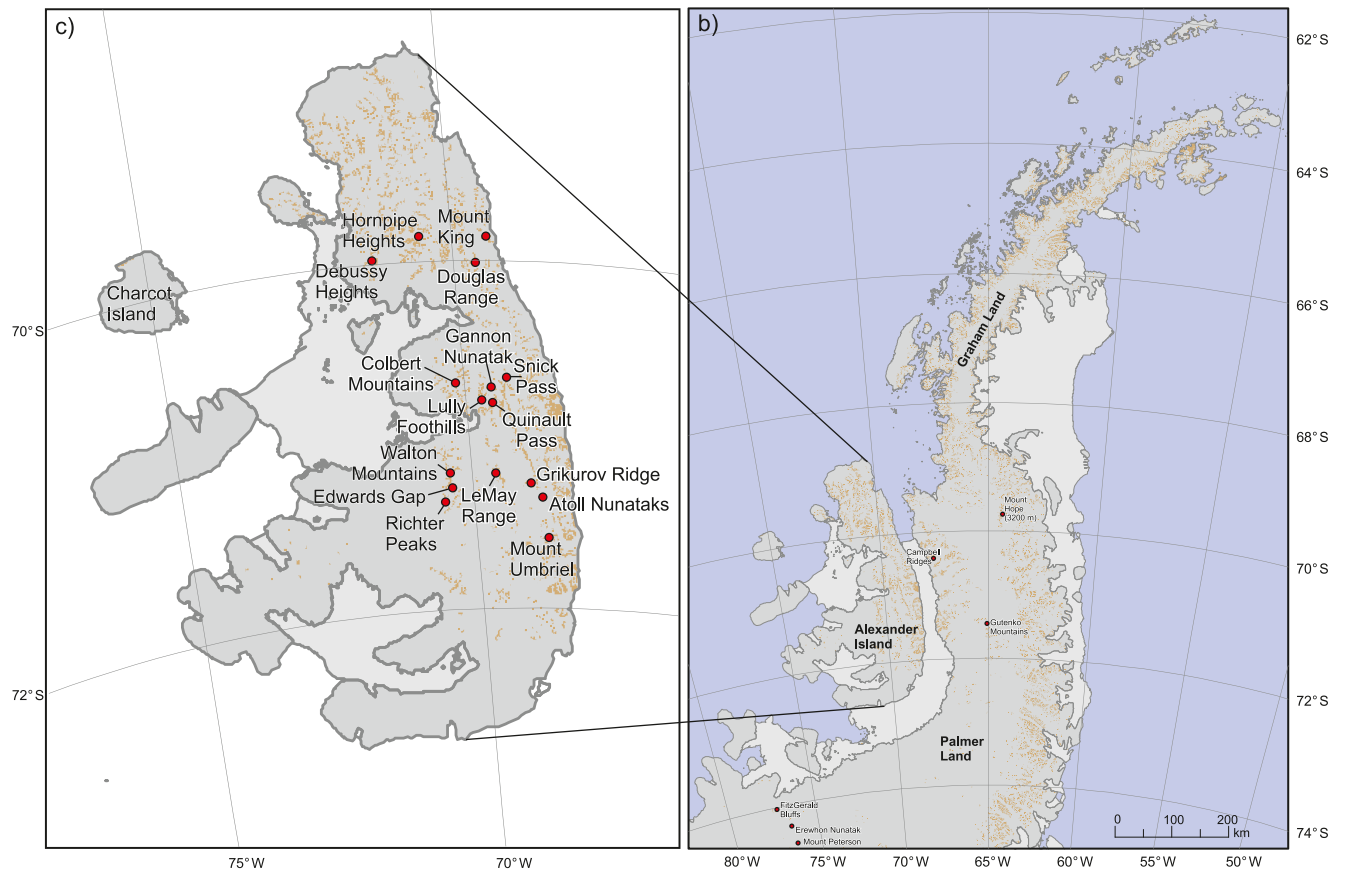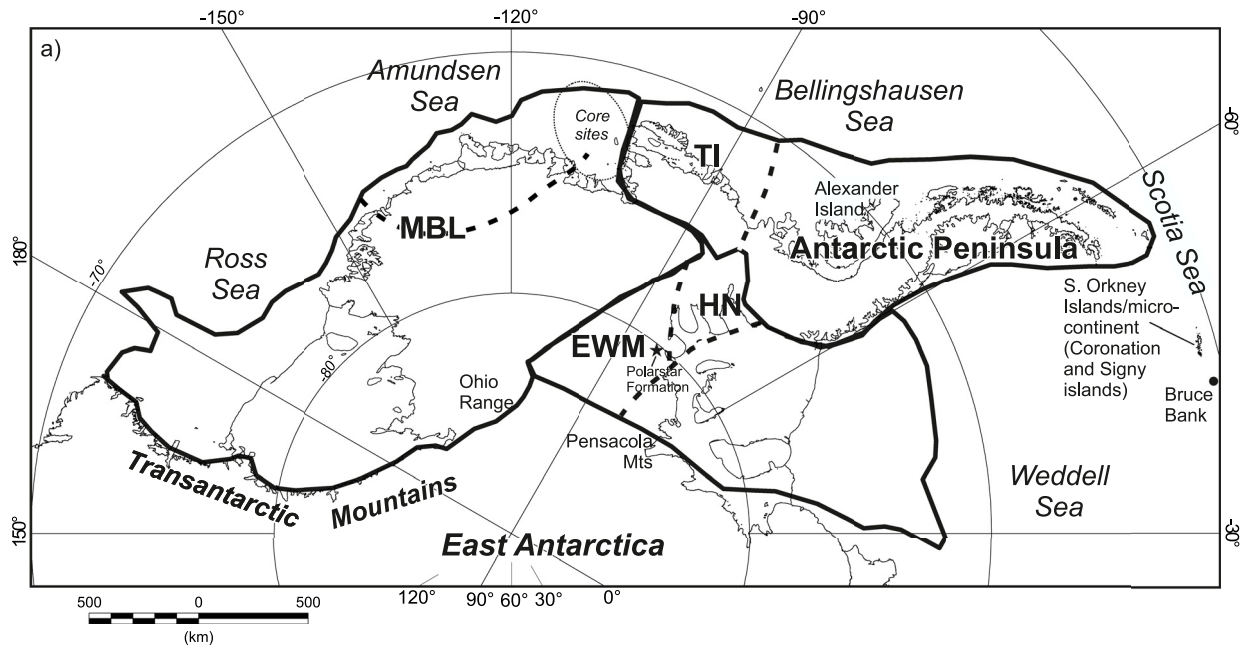
Figure 2. (a) Map of West Antarctica. EWM: Ellsworth-Whitmore Mountains; HN: Haag Nunataks; MBL: Marie Byrd Land; TI: Thurston Island. Core sites in the Amundsen Sea region are from Simões Pereira et al. (2018). (b) Map of the Antarctic Peninsula; (c) Map of Alexander Island. Maps generated in QGIS.
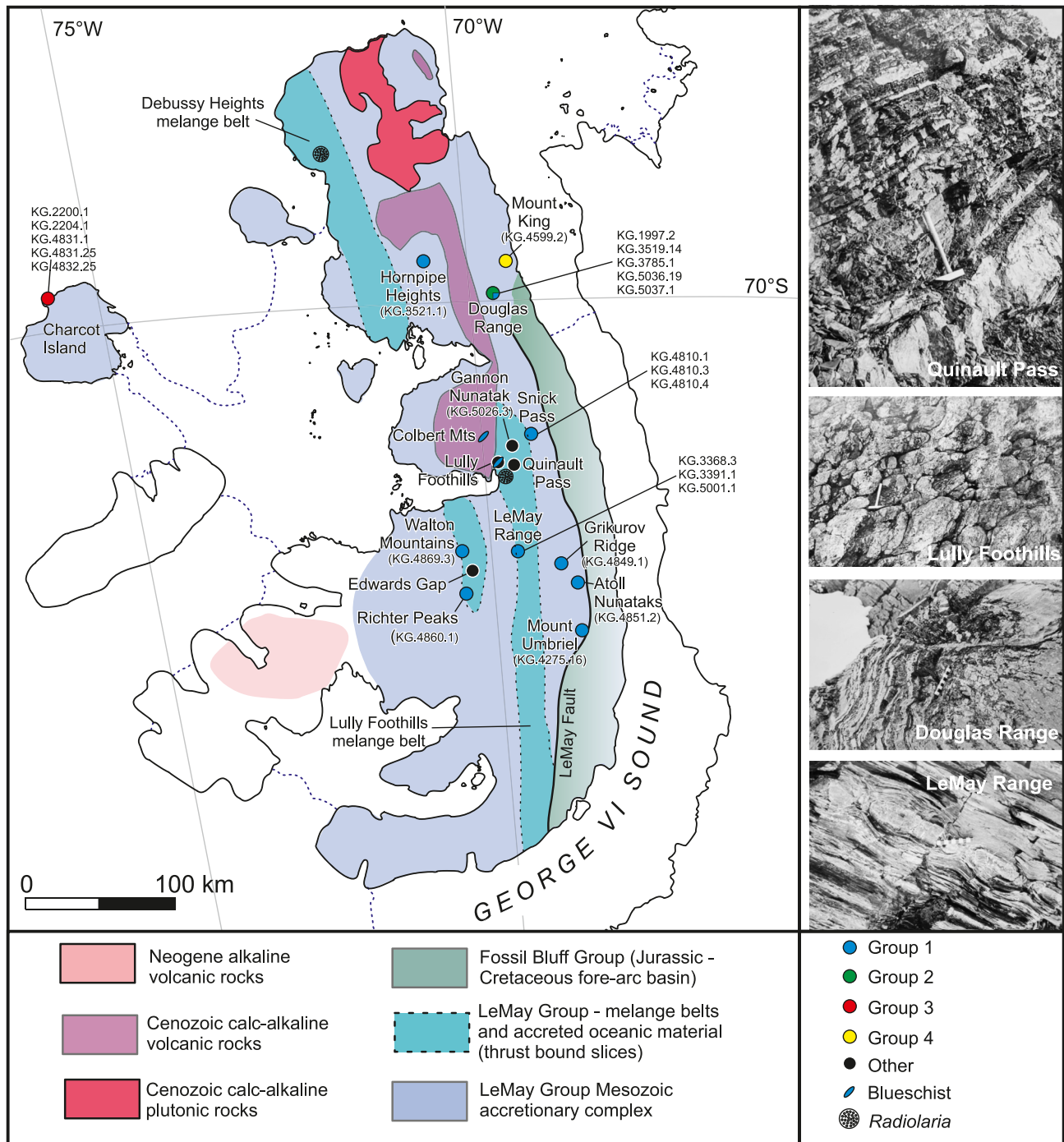
Figure 3. Geological map of Alexander Island showing LeMay Group sample sites and groupings based on the detrital zircon U-Pb age and Lu-Hf isotope systematics. Representative field photographs are from Tranter (1988) (a) typical mudstone-sandstone assemblage of the LeMay Group; (b) pillow basaltic lava from Lully Foothills; (c) F2 fold in thinly bedded sandstone and shale; (d) boudinage of sandstone in shale.

Tranter (1988) and Willan (2003) both used petrography and geochemistry to help understand the provenance of the LeMay Group sandstones. They suggested that they were derived from a deeply eroded continental margin with variable input from an active arc, likely to be from adjacent Palmer Land on the Antarctic Peninsula (Tranter, 1988). Willan (2003) also suggested that the bulk of the LeMay Group has modal compositions similar to the Permo-Triassic sequences of the Torlesse Supergroup in the Eastern Province of New Zealand, although the occurrence of Carboniferous magmatism in New Zealand is not consistent with the LeMay Group succession.

Willan (2003) also recognised that the Charcot Island sequences to the west of Alexander Island were distinct to the main LeMay Group succession and suggested an exotic paleoposition, potentially adjacent to Thurston Island (Figure 2a).

The components of ocean floor and ocean island that occur within the LeMay Group accretionary complex are interpreted to represent far-traveled fragments of proto-Pacific oceanic floor (Phoenix Plate and Bellingshausen Plate) that form thrust-bound allochthonous slivers (Doubleday et al., 1994). The accreted basaltic rocks occur at several locations within the LeMay Group (Burn, 1984) and crop out in two linear belts; the Debussy Heights mélange belt and the Lully Foothills mélange belt (Figure 3). The relationship between the accreted oceanic material and the sedimentary rocks of the accretionary prism is tectonic, with the basaltic lithologies and associated sedimentary rocks always occurring as thrust-bound slices. Doubleday et al. (1994) interpreted this relationship to indicate that the basalts were neither emplaced into the trench/fore-arc sector nor do they represent arc basement, but rather comprise more exotic ocean floor material. The basalt-chert units of the mélange belts are also associated with trench-fill arkosic sedimentary rocks that are not seen in direct contact with the basalts except where they are faulted. The geochemistry of the basaltic rocks was investigated by Doubleday et al. (1994) who demonstrated they were broadly MORB-like, although the Lully Foothills basalts are OIB-like and are interpreted as a remnant ocean island or seamount. The chert horizons associated with the accreted basaltic units (Holdsworth & Nell, 1992) yielded assemblages of Jurassic and Cretaceous *Radiolaria* indicative of an open ocean setting and their presence was used to suggest an allochthonous origin for at least parts of the LeMay Group accretionary complex, with docking not complete until c. 90 Ma. But there is uncertainty as to the origin of the chert units as either open ocean or near continent silica-rich beds (Holdsworth & Nell, 1992) and a Late Cretaceous docking age is not consistent with accretion models from elsewhere along the margin (e.g., South Orkney Islands; Flowerdew et al., 2007).

Storey et al. (1996) carried out a zircon and apatite fission-track analysis of a range of samples from the LeMay Group and identified a similar thermal history to the adjacent Fossil Bluff Group, with Cretaceous and Cenozoic thermal and denudational history, overlapping with Cretaceous deformation in a strike-slip setting. Twinn et al. (2022) also presented apatite fission track data from Alexander Island and Palmer Land, which was in broad agreement with Storey et al. (1996) and they identified late stage, rapid cooling at 25 Ma from the LeMay Range region.

2.4. Samples

Samples for detrital zircon and white mica analysis were selected from across a broad range of the LeMay Group to permit the most comprehensive analysis of the succession's provenance. Twenty-two samples (Figure 3; Table S1) were selected from Charcot Island in the west, to Mount King in the east and include several samples from the type areas of the LeMay Group, from the Douglas Range, Walton Mountains and LeMay Range (Figure 2; Tranter, 1988). Full positional information is provided in Table S1.

2.4.1. Douglas Range and Hornpipe Heights

The LeMay Group of the Douglas Range region is dominated by steeply dipping turbidites that have undergone major ocean-ward thrusting likely involving several kilometres of displacement (Nell, 1990).

Sample KG.3519.14 from western Douglas Range is a coarse greywacke from a west-directed thrust zone and is part of a duplex structure, which disrupts an earlier cleavage. Sample KG.3785.1 from the northwest Douglas Range is a sandstone from a massive turbidite sequence that dips steeply to the southwest. The beds exhibit primary sedimentary structures (e.g., graded bedding, load casts) and a weakly developed fabric is cut by later reverse faults. Sample KG.5036.19 is a sandstone from the southwest Douglas Range, close to Snick Pass. The beds are steeply dipping and are part of a deformed turbidite succession, associated with conglomerate beds. Sample KG.5037.1 is from a deformed and steeply dipping sandstone-mudstone succession to the north of Snick Pass in the southwest Douglas Range region. Sample KG.1997.2 is a fine-medium-grained sandstone from the eastern Douglas Range. Sample KG.3521.1 is a deformed coarse greywacke from the Hornpipe Heights region of northern Alexander Island. The sequences are cut by two generations of reverse faults.

2.4.2. Walton Mountains—LeMay Range—Mount Umbriel

The Walton Mountains and LeMay Range of central Alexander Island are adjacent to the mélange belt of the LeMay Group accretionary complex which includes trench-fill turbidites and associated basalt-chert sequences.

The mélange belt is interpreted from field observations to form a distinct geological and tectonic unit to the accretionary prism succession exposed in the Douglas Range (Tranter, 1988).

Sample KG.3391.1 is a deformed, steeply dipping sandstone from a sandstone-shale sequence from the southwest LeMay Range (Figure 3). The succession is broadly similar to those from the Douglas Range, but lacks conglomerate beds and are associated with pillow basalts (Figure 3) and more silicic-rich rocks associated with the mélange belt (Figure 3). Sample KG.4275.16 is a sandstone from Mount Umbriel, close to the boundary with the Fossil Bluff Group (Figure 3). It forms part of a weakly deformed sandstone-mudstone sequence. Sandstone sample KG.4869.3 also comes from a weakly deformed sandstone-mudstone sequence that preserves primary preserve sedimentary structures from the northeast Walton Mountains. The weakly deformed sequences strongly resemble those exposed from the LeMay Range. Sample KG.5001.1 comes from a sandstone interbed within a sandstone-conglomerate unit from the eastern LeMay Range, with the conglomerate beds characterized by abundant quartzite cobbles. Sample KG.3368.3 from the LeMay Range is a sandstone from a thick (few meters) band in a mostly siltstone-shale sequence. Sample KG.4860.1 is a coarse-grained sandstone from Richter Peaks in the southern part of the Walton Mountains (Figure 3).

2.4.3. Snick Pass, Grikurov Ridge and Atoll Nunataks

Snick Pass and Atoll Nunataks lie in the LeMay Group accretionary complex from a unit to the east of the mélange belt and to the west of the LeMay fault zone in contact with the Fossil Bluff Group (Figure 3).

Sample KG.4810.3 is a quartzite clast from a polymict conglomerate bed at Snick Pass and forms part of a conglomerate-sandstone-mudstone association. The conglomerate has abundant sub-rounded clasts of silicic volcanic rocks, quartzite, chert, vein quartz, sandstone, mudstone and rare plutonic clasts. Sample KG.4810.4 is a sandstone-conglomerate unit from the unit described above at Snick Pass. Sample KG.4810.1 is a coarse-grained sandstone unit from the main sandstone-conglomerate succession at Snick Pass. Sample KG.4851.2 is a coarse-grained quartz-rich sandstone from Atoll Nunataks from the eastern margins of the LeMay Group where an unconformable/faulted contact with the younger Fossil Bluff Group is exposed and may represent the oldest exposed part of the LeMay Group. Sample KG.4849.1 is a very coarse-grained sandstone/gritstone from Grikurov Ridge to the northwest of Atoll Nunataks (Figure 3).

2.4.4. Charcot Island

Charcot Island lies to the west of Alexander Island (Figure 3) and although it is mostly snow and ice-covered, isolated outcrops on the northwest coast expose the most westerly extent of the LeMay Group (Tranter, 1988). Samples KG.2200.1, KG.2204.1, KG.4831.1, KG.4831.25, and KG.4832.25 form part of a sandstone-conglomerate-shale turbidite succession with evidence of weak deformation and late-stage faulting.

2.4.5. Mount King

Mount King is located adjacent to King George VI Sound and lies at the eastern margin of the LeMay Group (Figure 3). The succession at Mount King is estimated to be 1 km in thickness and coarsens up from mudstone at its base to abundant sandstone-conglomerate units higher in the sequence. Locally, mudstone units are highly fossiliferous and preserve a diverse macrofauna of Carboniferous and Permian fossils (Kelly et al., 2001). Sample KG.4599.2 is a coarse-grained sandstone from a site located 4 km to the southeast of Mount King.

3. Objectives

This study has two primary objectives: (a) To determine the depositional age and provenance of the LeMay Group accretionary complex using a combination of U-Pb detrital zircon ages, Lu-Hf isotope and detrital white mica ages. (b) To use the new age and isotope data to explore the potential role of terrane translation along the proto-Pacific margin and whether the LeMay Group accretionary complex shares a geological affinity with the northern Antarctic Peninsula-Patagonia-Scotia Metamorphic Complex, West Antarctica/New Zealand, or if a dominantly autochthonous origin is more appropriate. We will investigate the detrital zircon age profiles of sedimentary successions from across southern Patagonia, Scotia Sea, Antarctic Peninsula, East Antarctica and New Zealand to help determine the provenance and tectonic history of the LeMay Group accretionary complex.

4. Analytical Methods

4.1. U-Pb Zircon Geochronology

Zircon (U-Pb) geochronology was carried out at five separate laboratories (Swedish Museum of Natural History, University College London, British Geological Survey, Australian National University and Trinity College Dublin) and full analytical procedures from each laboratory are provided in Supporting Information S1 and the data are presented in Table S2. The majority of the analyses were undertaken at the Swedish Museum of Natural History and University College London and a summary of the analytical procedures are detailed here.

At the Swedish Museum of Natural History (Stockholm) U-Pb ion-microprobe zircon geochronology was carried out using a CAMECA 1280 ion microprobe at the NordSIM facility. The analytical method closely followed Whitehouse and Kamber ([2005]), but differs insomuch that the oxygen ion primary beam was generated using a high-brightness, radiofrequency (RF) plasma ion source (Oregon Physics, Hyperion II, rather than a duoplasmatron) and a focused beam instead of illuminated aperture. The 10 nA O_2- beam was rastered over 5×5 μm to homogenize beam density, the final analytical spot size being c. 15 μm in diameter. Sputtered secondary ions introduced into the mass spectrometer were analyzed using a single ion counting electron multiplier over 10 cycles of data. Data were reduced using in-house developed software. The power law relationship between $^{206}Pb/^{238}U^{16}O$ and $^{238}U^{16}O_2/^{238}U^{16}O$ measured from the 91500 standard was used to calibrate U/Pb ratios following the recommendations of Jeon and Whitehouse ([2015]). Common-Pb corrections were applied to analyses where statistically significant ^{204}Pb was detected, using the present-day terrestrial common Pb estimate of Stacey and Kramers ([1975]). Terra-Wasserburg U-Pb concordia diagrams were drawn using Isoplot v. 4.15 (Ludwig, [2012]). ^{207}Pb corrected ages were calculated assuming non-radiogenic Pb was from surface contamination and had an isotopic composition of modern-day average terrestrial common Pb ($^{207}Pb/^{206}Pb = 0.836$; Stacey & Kramers, [1975]).

Zircon U–Pb geochronology at University College London was carried out using laser ablation inductively coupled mass spectrometry (LA-ICP-MS) facilities (Agilent 7700 coupled to a New Wave Research 193 nm excimer laser) at the London Geochronology Centre. Typical laser spot sizes of 25 μm were used with a 7–10 Hz repetition rate and a fluence of 2.5 J/cm². Background measurement before ablation lasted 15 s and laser ablation dwell time was 25 s. The external zircon standard was Plešovice, which has a TIMS reference age 337.13 ± 0.37 Ma (Sláma et al., [2008]). Standard errors on isotope ratios and ages include the standard deviation of $^{206}Pb/^{238}U$ ages of the Plešovice standard zircon. Time-resolved signals that record isotopic ratios with depth in each crystal were processed using GLITTER 4.5, data reduction software, developed by the ARC National Key Center for Geochemical Evolution and Metallogeny of Continents (GEMOC) at Macquarie University and CSIRO Exploration and Mining. Processing enabled filtering to remove spurious signals owing to overgrowth boundaries, weathering, inclusions, or fractures. Ages were calculated using the $^{206}Pb/^{238}U$ ratios for samples dated as <1.1 Ga, and the $^{207}Pb/^{206}Pb$ ratios was used for older grains. Discordance was determined using (($^{207}Pb/^{235}U$ − $^{206}Pb/^{238}U$)/$^{206}Pb/^{238}U$) and similar for $^{207}Pb/^{206}Pb$ ages.

4.2. Lu-Hf Isotope Analysis

Lu-Hf isotopes were determined on a subset of those zircons analyzed for their U-Pb age using the same analytical spot to provide additional provenance information to support the U-Pb geochronology. The analyses were determined on a Neptune multi-collector inductively coupled plasma—mass spectrometer (ICP-MS) coupled with a laser ablation system at the British Geological Survey (UK). Initial $^{176}Hf/^{177}Hf$ ratios were calculated using the U-Pb crystallisation age of each grain and the results are expressed as initial εHf (εHf$_i$). εHf values were calculated using a ^{176}Lu decay constant of $1.867 \times 10^{-11} yr^{-1}$ (Söderlund et al., [2004]), the present-day chondritic $^{176}Lu/^{177}Hf$ value of 0.0336 and $^{176}Hf/^{177}Hf$ ratio of 0.282785 (Bouvier et al., [2008]). Full analytical details are provided in the Supporting Information S1 and the data are presented in Table S3.

4.3. Detrital White Mica Analysis

Detrital mica age distributions were determined from two samples from Grikurov Ridge and Charcot Island (Figure 3) tp provide additional geochronological control and information on the deformation history of the LeMay Group. $^{40}Ar/^{39}Ar$ detrital mica data were carried out at the Open University and full analytical details are provided in Supporting Information S1 and the data are presented in Supplementary Table S4.

5. Results

5.1. U-Pb Detrital Zircon Geochronology

Twenty-one samples (Table S1) from across the entire extent of the LeMay Group accretionary complex were selected for U-Pb detrital zircon geochronology. The most striking aspect of the data is the significant variation across the LeMay Group from eastern Alexander Island to Charcot Island in the northwest.

The age distribution of all 21 samples are plotted in Figure 4 as kernel density estimates (after Vermeesch, 2018), except where analysis numbers are <50 (six samples) and probability density plots are also shown to permit an additional layer of granularity. Three distinct age distributions are evident across the LeMay Group (Figure 5) which have a broadly spatial distribution (Figure 3). The main succession of the LeMay Group exposed in central Alexander Island (e.g., LeMay Range and Walton Mountains) is characterized by two primary age peaks at c. 253 Ma and c. 531 Ma, along with a broad distribution of Neoproterozoic ages and is defined as Group 1 (Figure 5). The samples analyzed from the Douglas Range region of northern Alexander Island have a distinct age distribution to the LeMay Range-Walton Mountains area. A Late Permian age peak of c. 262 Ma is akin to the LeMay Group of central Alexander Island, but the age distribution from the Douglas Range lacks the prominent Early Cambrian age peak (c. 530 Ma) and is defined as Group 2 (Figure 5). The samples from the Douglas Range sequence do have a minor Ordovician peak at c. 470 Ma, which is also identified in the central Alexander Island distribution (Group 1). The age distribution of the LeMay Group succession from Charcot Island (Group 3) is distinct to both Groups 1 and 2. The Charcot Island (Group 3) sequence is anticipated from field observations to be the youngest part of the LeMay Group succession (Tranter, 1988). This is borne out by the age distribution (Figure 5) which is characterized by a prominent Early Jurassic age peak (c. 185 Ma), but also with a minor, but significant mid-Cretaceous (c. 121 Ma) age peak. An Ordovician—Cambrian population is also evident from Charcot Island, akin to Groups 1 and 2, as well as a broad distribution of Neoproterozoic ages. The four samples from Charcot Island are also characterized by a greater population (c. 10%) of ages >1,200 Ma relative to the other successions of the LeMay Group (Figure 4). A noteworthy characteristic from the Group 3 sequences at Charcot Island is the complete absence of a Late Permian age peak (c. 260 Ma) that is the key feature of the LeMay Group elsewhere on Alexander Island (Figure 5).

Five samples from the LeMay Group of Alexander Island do not fit the criteria of Groups 1–3. Sample KG.4860.1 (Figure 4t) from Richter Peaks (Figure 3) is essentially akin to the age distributions that characterize Group 1, but in addition has a prominent Late Jurassic (c. 148 Ma) peak alongside the Permian (c. 262 Ma) and Cambrian (c. 528 Ma) age peaks. The conglomerate beds from Snick Pass (Figure 3) exhibit distinct age profiles; a quartz-ite clast (Figure 4r; KG.4810.3) has prominent Cambrian (c. 542 Ma) and Mesoproterozoic (c. 1,038 Ma) age peaks, but lacks any Permian grains. The conglomerate (KG.4810.4; Figure 4s) has a more complex age profile reflecting a matrix that has incorporated the signatures of some of the clasts. A silicic volcanic tuff was also analyzed from Gannon Nunatak (Figure 3) to determine the age of volcanism from central Alexander Island. The tuff (KG.5026.3; Figure 4v) has a prominent zircon population at c. 118 Ma, which is interpreted as the age of volcanism (see Figure S1 in Supporting Information S1).

A single sample (KG.4599.2) from Mount King (Figure 3) was also investigated, which from field observations is distinct to the main LeMay Group accretionary complex (Kelly et al., 2001). This is also borne out in the detri-tal zircon age profile which has a prominent Triassic peak at c. 225 Ma (Figure 4u), distinct to all other LeMay Group units and, although only defined by one sample, is termed Group 4.

5.2. Lu-Hf Isotopes

Lu-Hf isotope analysis was carried out on a subset of the LeMay Group samples analyzed for U-Pb geochronology. Seven samples were selected for analysis from each of the four groups identified from the U-Pb age profiles and all zircon grains analyzed for U-Pb geochronology were also selected for Lu-Hf analysis (Table S3).

Two samples (KG.3391.1; KG.4275.16) from Group 1 yield a broad scatter of εHf_i values across the entire age population (Figure 6a). The Late Permian (c. 253 Ma) age population has εHf_i values typically in the range −2 to −6. The other prominent age peak in the Early Cambrian (c. 531 Ma) has εHf_i values in the range −1 to −5, akin to the Late Permian age population.

Two samples (KG.3785.1; KG.3519.14) from the Douglas Range (Group 2) have a dominant age peak at c. 262 Ma that yields a far broader range of εHf_i values (+2 to −4; Figure 6) compared to the Group 1 rocks from the
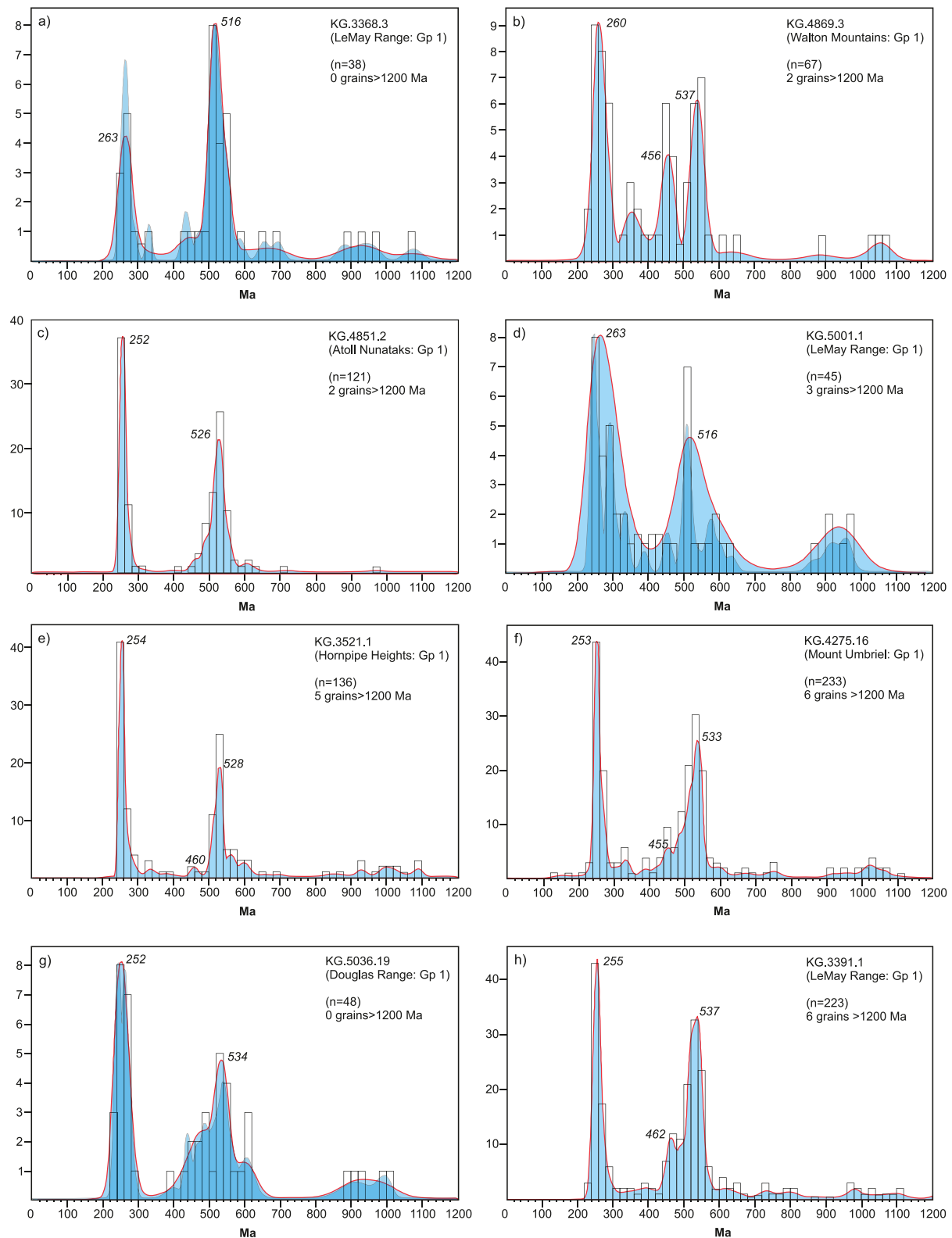
Figure 4. Kernel density estimator (KDE) and relative probability density (where *n* < 50) plots for a range of sandstone lithologies from the LeMay Group accretionary complex. The darker blue shading is for the probability density curve where *n* < 50 and underlies the KDE curve. Full datasets are available in Table S2. A fixed bandwidth is not appropriate for detrital zircon data which is strongly multimodal. As a result KDEs are generated here by default using an "adaptive" bandwidth which varies the bandwidth according to the density of points (see Vermeesch et al., 2016). Binwidths for all plotted samples are 20 Ma.
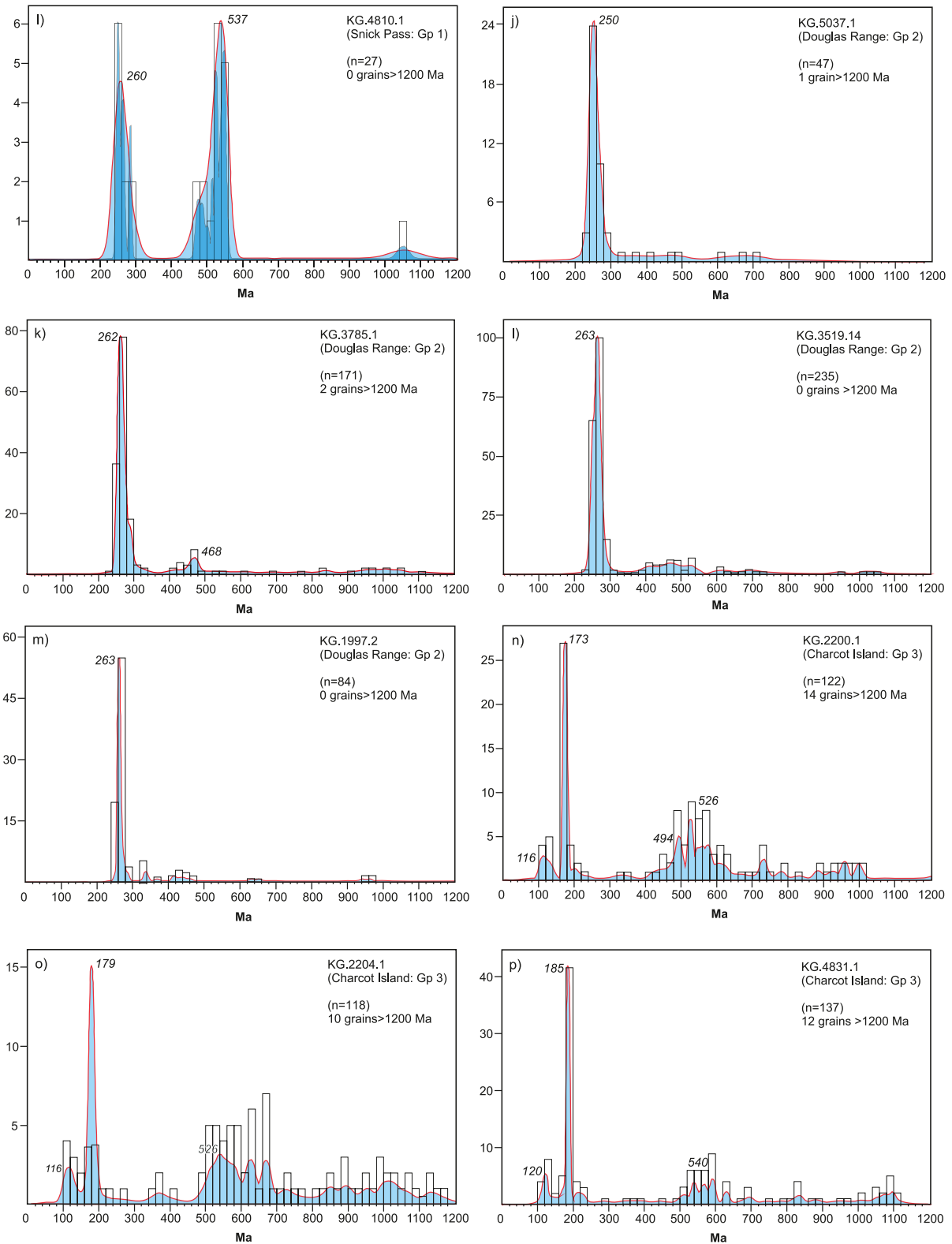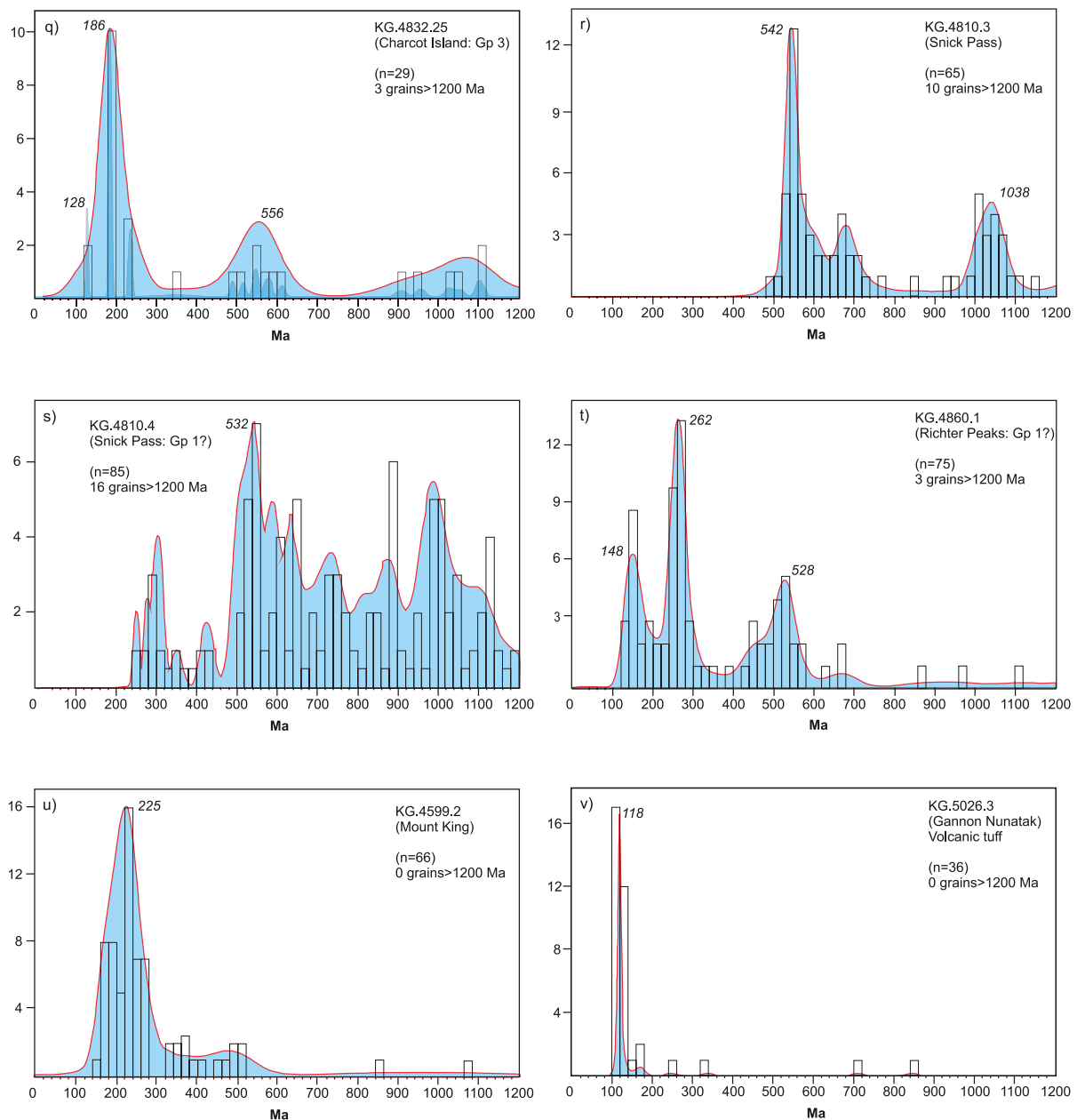
Figure 4. (Continued)

Figure 4. (Continued)

LeMay Range region. The Ordovician age (c. 470 Ma) detrital zircons characteristic of Group 2 have εHf_i values typically in the range +4 to 0. These values are generally more positive in comparison to the Ordovician ages from the LeMay Range area of Group 1, but are broadly akin to the Ordovician εHf_i values (+2 to −4) reported from the Trinity Peninsula Group (Figure 6b; Castillo et al., 2016).

Two samples from Charcot Island (Group 3) were also analyzed (KG.4831.1; KG.4832.25) for Lu-Hf isotopes. The primary age peak at c. 185 Ma yields a relatively narrow range of εHf_i vales of −8 to −11. The mid-Cretaceous ages are only evident in the Charcot Island (Group 3) sequences of the LeMay Group. They yield εHf_i values typically in the range −2 to −6 (Figure 6). The Early Cambrian age peak, also characteristic of the Charcot Island sample exhibit a very broad range in εHf_i values, but mostly within the range 0 to −4, akin to Group 1.

A single sample from Group 4 Mount King (KG.4599.2; Figure 3) was also investigated and yields a broad scatter in εHf_i values (0 to −10; Figure 6) for the Jurassic to Permian age grains. The Jurassic range, 0 to −5 is distinct
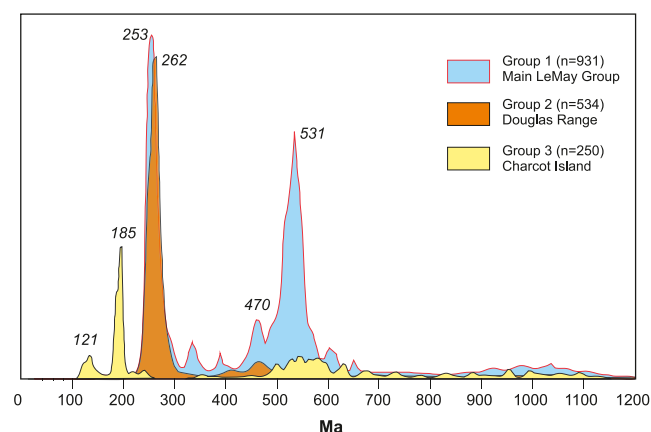
Figure 5. Kernel density estimator plot for Groups 1–3 from the LeMay Group accretionary complex. *n* = number of analyses.

to the Charcot Island (Group 3) Jurassic εHf_i values, which are considerably more radiogenic (−8 to −11).

5.3. Detrital White Mica Ages

Two samples were selected for detrital white mica $^{40}Ar/^{39}Ar$ analysis (Table S4) to help understand the thermal, accretion and deformational history of the LeMay Group. One sample (KG.4849.1) from Grikurov Ridge is likely to be part of Group 1, whilst the other sample (KG.4831.25) is from the sequences exposed in northwest Charcot Island (Group 3).

Sixteen grains of detrital white mica from the Grikurov Ridge siltstone (KG.4849.1; Figure 7) yielded a narrow range of $^{40}Ar/^{39}Ar$ ages from 231.8 ± 4.0 Ma to 266.8 ± 15.0 Ma (2σ errors). Fifteen analyses were carried out on detrital white mica grains from a Group 3 (Charcot Island) siltstone (KG.4831.25; Figure 7). Fourteen analyses yielded a narrow range of $^{40}Ar/^{39}Ar$ ages from 98.2 ± 8.8 Ma to 117.3 ± 2.4 Ma (2σ errors). A single mica analysis gave an older age of 186 ± 2 Ma (2σ error; Figure 7).

6. LeMay Group Provenance Analysis

The comprehensive geochronological and geochemical data set from the LeMay Group of Alexander Island permits a provenance and depositional history analysis of an accretionary complex during dynamic continental margin convergence. A comparison with sedimentary units from the Antarctic Peninsula, East Antarctica, Patagonia, the Scotia Metamorphic Complex and the Torlesse terrane accretionary complex of the New Zealand Eastern Province is presented to evaluate the potential contribution of exotic terranes to the assembly and the tectonic history of Alexander Island.

6.1. Comparative Units

Late Paleozoic and Mesozoic sedimentary and metasedimentary units from, or adjacent to the proto-Pacific margin of West Gondwana (Figure 8) are summarized here to evaluate their relationship to the LeMay Group accretionary complex as potential correlative or source units.

6.1.1. Northern Antarctic Peninsula (Graham Land)

The geology of the northern Antarctic Peninsula is dominated by the Carboniferous—Triassic Trinity Peninsula Group (Figure 1). It is a 4–5 km succession of variably deformed siliciclastic turbidites with rare interbedded mafic volcanic rocks (Hyden & Tanner, 1981), which has been correlated with the metaturbidites of the Permian Duque de York Complex of southern Patagonia (Sepúlveda et al., 2010). The Trinity Peninsula Group was deposited in a continental margin fore-arc setting from the mid-Carboniferous to the Triassic (Bradshaw et al., 2012) with part of the succession deposited onto crystalline continental basement (Hervé et al., 1996). The entire succession was incorporated into an accretionary complex with outboard correlatives in the Scotia Metamorphic Complex (Trouw et al., 1998) and Greywacke Shale Formation (Trouw et al. (1997)) forming part of the South Orkney microcontinent (Figure 2a). The Miers Bluff Formation (Figure 1) was initially considered a correlative of the Trinity Peninsula Group but U-Pb detrital zircon ages indicate deposition of the Miers Bluff Formation post-dated the Middle Jurassic (Hervé et al., 2006).

The Trinity Peninsula Group has been subdivided into six separate formations across northern Graham Land, although only three successions (Figure 1) have a well-defined stratigraphy; View Point Formation (Carboniferous—Early Permian; Bradshaw et al., 2012), Hope Bay Formation (Triassic turbidite succession; Birkenmajer, 1992) and the Legoupil Formation (Permian—Triassic quartz arenites; Thomson, 1975) of western Graham Land.

Several studies have examined the detrital zircon age population of the Trinity Peninsula Group (Barbeau et al., 2010; Bradshaw et al., 2012; Castillo et al., 2015, 2016; Fanning et al., 2011). These investigations identified a dominant Permian age of source material and likely depositional age, but many sections of the Trinity Peninsula
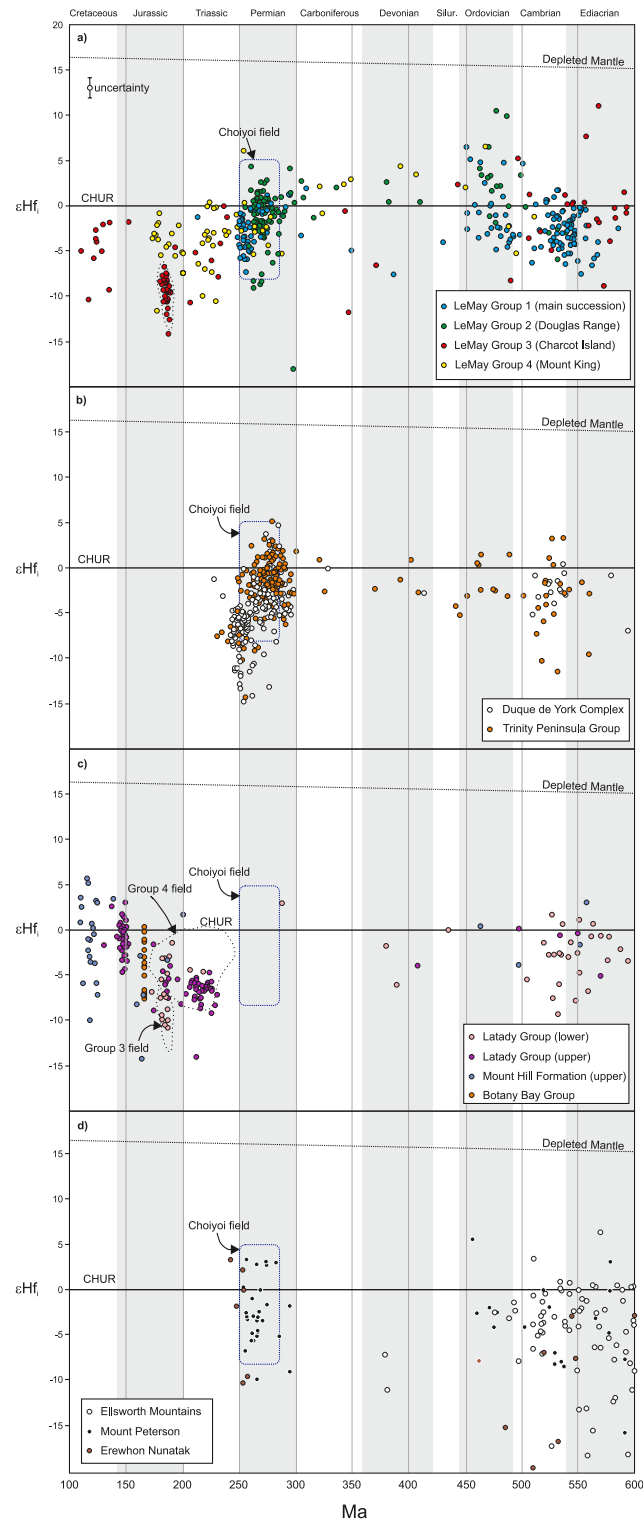
Figure 6. U–Pb zircon ages (^{238}U/^{206}Pb) versus initial εHf values for zircon grains analyzed in this study (Table S3). (a) LeMay Group accretionary complex (this study); (b) Trinity Peninsula Group and Duque de York Complex (Barbeau et al., 2010; Bradshaw et al., 2012; Castillo et al., 2015, 2016; Fanning et al., 2011); (c) Antarctic Peninsula sedimentary successions (BAS unpublished data); (d) Ellsworth Mountains, Mount Peterson and Erewhon Nunatak (Elliot et al., 2016; BAS unpublished data). Group 1: KG.3391.1, KG.4275.16; Group 2: KG.2519.14, KG.3785.1; Group 3: KG.4831.1, KG.4832.25; Group 4: KG.4599.2.

Figure 7. Probability density plot showing the distribution of ^{40}Ar-^{39}Ar ages on detrital white mica from Group 1 (Grikurov Ridge) and Group 3 (Charcot Island). Peak maxima ages are approximations.

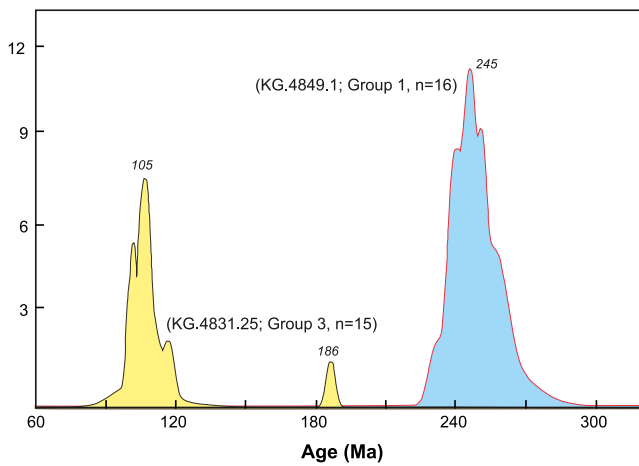Group also exhibit Ordovician and to a lesser extent, Carboniferous age peaks (Figure 9). The Trinity Peninsula Group succession at View Point from northern Graham Land (Figure 1) was examined by Bradshaw et al. (2012) and yields a distinct detrital zircon age profile to units from elsewhere in the Trinity Peninsula Group. The View Point sandstone-conglomerate succession lacks the prominent Permian age zircons identified throughout other units of the Trinity Peninsula Group (Figure 9). Bradshaw et al. (2012) determined a Lower Carboniferous likely depositional age of 302 ± 3 Ma, and potentially representing the oldest exposed sequence of the Trinity Peninsula Group.

Elsewhere in the northern Antarctic Peninsula, the Botany Bay Group (Figure 1) crops out along the east coast of northern Graham Land (Hunter et al., 2005). The succession consists of non-marine conglomerates, sandstones and mudstones with abundant plant fossils. The terrestrial sedimentary rocks of the Botany Bay Group record the initiation of extension that preceded the opening of the Weddell Sea (Figure 1). The Botany Bay Group has a depositional age of c. 167 Ma with a dominant detrital zircon age population of Middle Jurassic grains (Figure 9) with rarer Permian and Carboniferous ages (Hunter et al., 2005).

6.1.2. Southern Antarctic Peninsula (Palmer Land)

Several successions from the southern Antarctic Peninsula with depositional histories from the Late Paleozoic to Mesozoic are described here as potential comparative units to the LeMay Group accretionary complex. The most prominent unit is the Latady Group sedimentary succession of southern Palmer Land (Figure 1). The Latady Group has been subdivided into five separate formations (Hunter & Cantrill, 2006) with deposition in a rifted margin setting throughout the Jurassic. The sedimentary units reflect deposition in a range of environments from coastal to deep outer shelf marine and forms a succession several kilometres in thickness. The primary source to the Latady Group sedimentary basin is likely to be from the broadly contemporaneous Mount Poster Formation silicic volcanism of caldera-fed ignimbrite-forming eruptions (Hunter et al., 2006). There is no published detrital zircon data from the Latady Group succession, but unpublished British Antarctic Survey (BAS) data presented in Figure 9 (summarized in
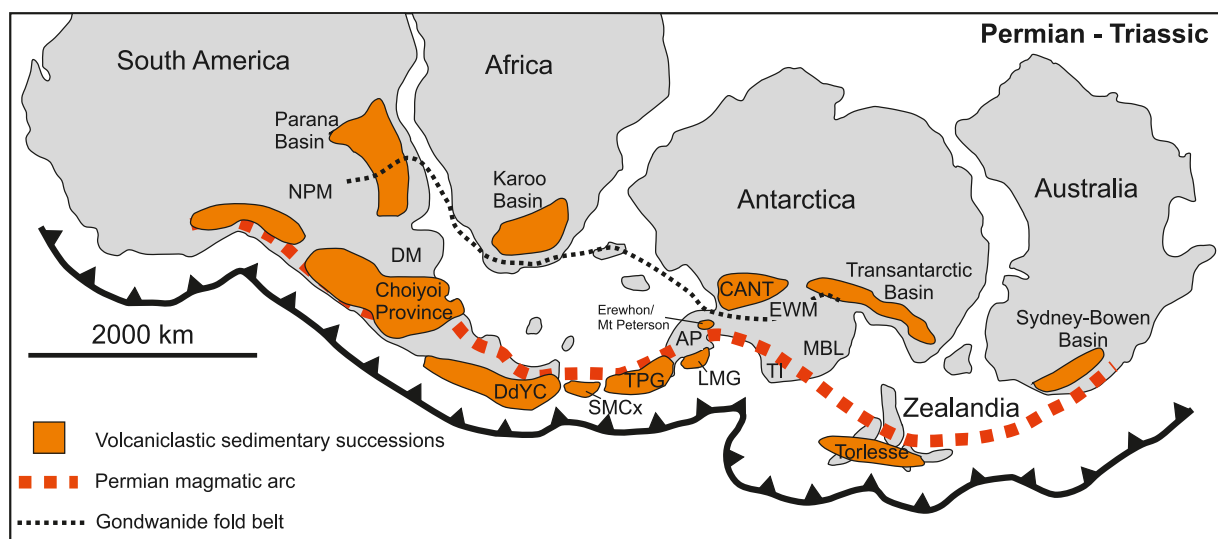
Figure 8. Reconstruction of the Permian—Triassic Gondwana continental margin highlighting the volcaniclastic sedimentary successions and magmatic arc front (adapted from Nelson & Cottle, 2019). The extent of the Gondwanide fold belt is from Eagles and Eisermann (2020). AP: Antarctic Peninsula; CANT: Central Antarctica; TI: Thurston Island; MBL: Marie Byrd Land; EWM: Ellsworth-Whitmore Mountains; NPM: North Patagonian Massif; DM: Deseado Massif; DdYC: Duque de York Complex; TPG: Trinity Peninsula Group; LMG: LeMay Group; SMCx: Scotia metamorphic complex.

Figure 9. Ridge plot age distributions (U–Pb zircon ages—^{238}U/^{206}Pb) for samples from the West Gondwana margin plotted in comparison to the LeMay Group age distributions (in bold). Data sources are provided in Table S5. The colors correspond to the ornament used in Figure 10 and the samples are plotted in order of similarity. SMCx: Scotia Metamorphic Complex; SSR: South Scotia Ridge.

Table S5) indicate a prominent Early Jurassic age peak, identical to the eruption age of the Mount Poster Formation (c. 183 Ma; Pankhurst et al., 2000; Hunter et al., 2006).
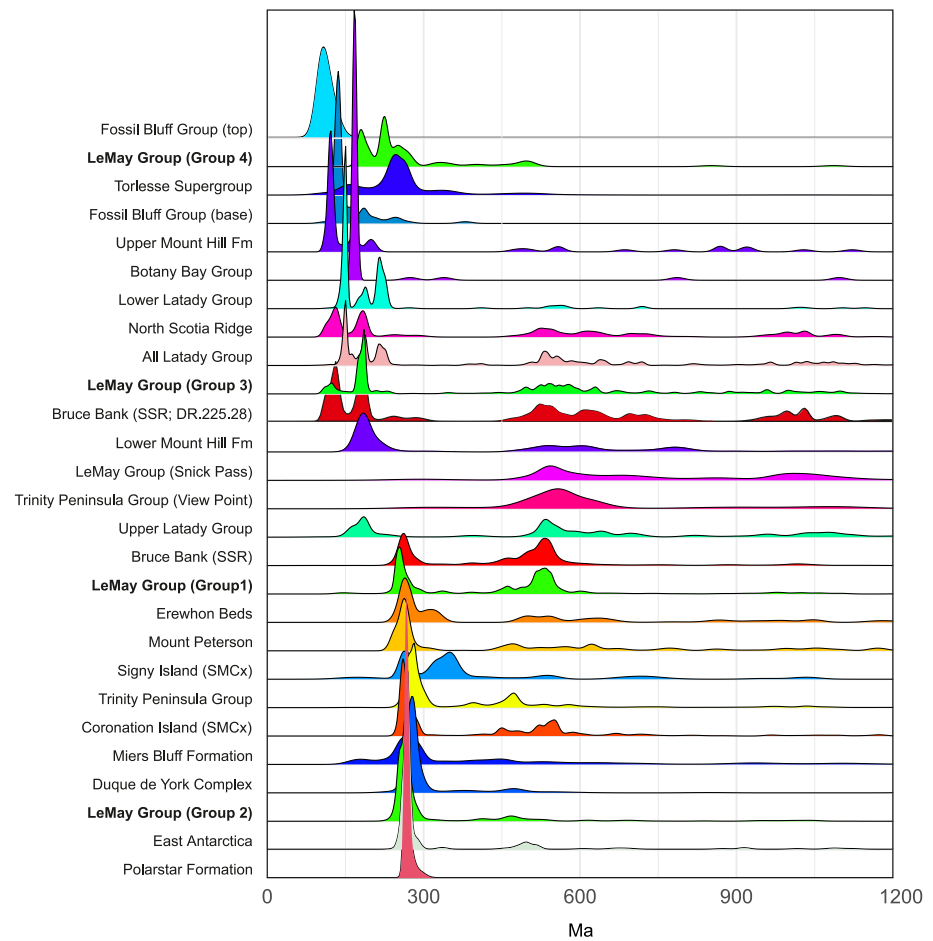
A potential correlative to the Latady Group-Mount Poster Formation sedimentary-volcanic succession is the Mount Hill Formation-Brennecke Formation units of eastern Palmer Land (Figure 1) where Early Jurassic volcanism (c. 184 Ma; Pankhurst et al., 2000) is considered broadly contemporaneous with the deformed metaturbidites of the Mount Hill Formation. There is no published detrital zircon data from the Mount Hill Formation but BAS unpublished data (summarized in Table S5) shown in Figure 9 identifies a much younger age of likely deposition (mid-Cretaceous), but with some input from an Early Jurassic source.

The basement geology to the Latady Group in southern Palmer Land was considered by Hunter and Cantrill (2006) to be the quartz-rich sandstones exposed at Erewhon Nunatak and FitzGerald Bluffs (Fig, 1). *Glossopteris* flora from Erewhon Nunatak, combined with detrital zircon analysis by Elliot et al. (2016) suggests a dominant Late Permian depositional age. Also shown in Figure 9 is the detrital zircon age profile (BAS unpublished data; Table S5) from Mount Peterson (Figure 9), adjacent to Erewhon Nunatak, which shows a very similar age population. The FitzGerald Bluffs quartzite beds are likely to be Devonian in age based on their detrital zircon age profile (Elliot et al., 2016) with a strong resemblance to the Crashite Group and quartz-rich sandstones of the Transantarctic Mountains (Figure 2).

The geology of the Erewhon Nunatak-Mount Peterson-FitzGerald Bluffs area of southern Palmer Land (Figure 1) is unusual for a continental margin setting and Elliot et al. (2016) regarded them as part of a small allochthonous

Figure 10. Multidimensional scaling maps (MDS; Vermeesch, 2018) comparing the age spectra in dissimilar samples calculated using the Kolmogorov-Smirnov statistic. A MDS plot maps the degree of similarity between each sample, with any two points plotting closer if they are more similar. The axis scales are dimensionless and have no physical meaning. Individual sample MDS analysis from which the groupings are derived are provided in Figure S3 in Supporting Information S1. (a) MDS plot for all ages and (b) for ages <300 Ma. Full datasets and data sources are provided in Table S5. The Amundsen Sea data from Simões Pereira et al. (2018) is ⁴⁰Ar/³⁹Ar (hornblende and biotite) detrital data with all post-accretion ages (<90 Ma) disregarded. Numbers in parentheses are number of analyses. TPG: Trinity Peninsula Group; DdYCx: Duque de York Complex.

crustal block displaced from its original position adjacent to the Ellsworth Mountains or Transantarctic Mountains (Figure 2). Tranter (1988) reported conglomerate beds from the LeMay Group that contained abundant quartzite clasts (e.g., KG.4810.3) that may have been derived from Erewhon-FitzGerald crustal block.

The most proximal sedimentary unit to the LeMay Group accretionary complex is the neighboring Fossil Bluff Group of eastern Alexander Island (Figure 1). The Fossil Bluff Group is a Jurassic—Cretaceous fore-arc succession at least 7 km in thickness (Butterworth et al., 1988) that either lies unconformably above the LeMay Group or is in faulted contact. There is no published detrital zircon data from the Fossil Bluff Group, however unpublished data (summarized in Table S5) from the upper and lower parts of the succession exhibit a mid-Cretaceous only signature for the upper parts of the succession (Figure 9) and a prominent Late Jurassic—Early Cretaceous profile for the lower parts of the succession, alongside Early Jurassic and Triassic age populations.

6.1.3. East Antarctica and Ellsworth Mountains

A full comparative analysis with lithologies from East Antarctica is not appropriate for the LeMay Group accretionary complex given their distal relationship. However detrital zircon age data from the Permian Polarstar Formation of the more proximal Ellsworth Mountains (Figure 2) is shown in Figure 9 (Elliot et al., 2016; Nelson & Cottle, 2018), as are quartz-rich sandstones from the central Transantarctic Mountains (Nelson & Cottle, 2018). The Polarstar Formation is the youngest unit of the Ellsworth Mountains Paleozoic succession and it has been correlated with Permian units from the southern Antarctic Peninsula (Erewhon Beds), the Karoo (southern Africa), the Falkland Islands and central Transantarctic Mountains (Elliot et al., 2016). The Polarstar Formation has a detrital zircon age profile with a prominent Permian (c. 267 Ma) peak that Elliot et al. (2016) suggested were sourced from magmatism in Thurston Island or southern Palmer Land (Figure 2).

Comparable Permian units from the Ohio Range of the central Transantarctic Mountains and the Pecora Formation of the Pensacola Mountains (Figure 2) were examined by Nelson and Cottle (2018) and also yield major Permian age peaks of c. 270 Ma, which they correlated with the extensive Permian Choiyoi magmatic province (Figure 8).

6.1.4. Thurston Island

Although there are no sedimentary units exposed in Thurston Island (Figure 2) its proximity to the proto-Pacific margin and the Antarctic Peninsula mean that a geological summary would be of value. Riley et al. (2017) and Nelson and Cottle (2018) presented an updated chronology of the Thurston Island crustal block which has allowed more confident correlations to be drawn to adjacent crustal units elsewhere along the proto-Pacific margin of Gondwana. The oldest unit known in Thurston Island is a granodiorite orthogneiss which has been dated at 349 ± 2 Ma (Riley et al., 2017) and may form an extension of Devonian—Carboniferous magmatism in Marie Byrd Land and the Median Batholith of New Zealand. Triassic magmatism is recognised from the Antarctic Peninsula, Marie Byrd Land and New Zealand and is also identified from Thurston Island (239 ± 4 Ma; Riley et al., 2017) and are interpreted as melts with a major lower crustal component with extraction from a Mesoproterozoic source similar to those exposed at Haag Nunataks (Figure 2). Jurassic silicic volcanism from Thurston Island is dated at c. 182 Ma (Riley et al., 2017) and is interpreted as a direct correlative unit to the c. 183 Ma Brennecke and Mount Poster formations from the southern Antarctic Peninsula, which are part of the wider Chon Aike Province V1 event exposed extensively in Patagonia and the Antarctic Peninsula (Pankhurst et al., 2000). The most extensive phase of magmatism along the entire proto-Pacific margin occurred during the mid-Cretaceous, with a magmatic peak in the interval 118–105 Ma (Riley et al., 2018). Granitoid magmatism of this period, preserved as extensive batholiths, occurred from Patagonia to southeast Australia, including Thurston Island (Riley et al., 2017). It marks a major Cordillera 'flare-up' event characterized by high magma intrusion rates as over-thickened lithosphere was extended and potentially melted.

Shallow sediment cores taken from the Amundsen Sea-Bellingshausen Sea (Figure 2) region adjacent to Thurston Island have been examined for their detrital biotite and hornblende age populations (Simões Pereira et al., 2018) and multiple core sites all show prominent mid-Cretaceous (c. 110 Ma) and Middle Jurassic (c. 170 Ma) age peaks.

6.1.5. Scotia Sea Area

Several units from the Scotia Sea (Figure 2a) area were also selected for comparison to the LeMay Group accretionary complex. The Scotia Metamorphic Complex is a highly deformed metasedimentary wedge, which contains a significant proportion of ocean floor material (Dalziel, 2013; Trouw et al., 1997), and has a geological and accretional history from the Late Paleozoic to the Cenozoic. The Scotia Metamorphic Complex is exposed from the South Shetland Islands (Trouw et al., 1997), along the South Scotia Ridge (Bruce Bank; Riley, Carter,

et al., 2022; Riley, Burton-Johnson, et al., 2022) to the South Orkney Islands (Flowerdew et al., 2011), including Permian—Triassic metasedimentary rocks from Signy Island and Coronation Island (Figure 2). The units of the Scotia Metamorphic Complex and correlative Greywacke Shale Formation (South Orkney Islands) all have prominent Permian zircon U-Pb age peaks at c. 265 Ma and Cambrian peaks at c. 530 Ma (Carter et al., 2017; Riley, Carter, et al., 2022; Riley, Burton-Johnson, et al., 2022). White mica that forms the pervasive foliation within the Scotia Metamorphic Complex has been dated at c. 190 Ma by Flowerdew et al. (2007).

The Miers Bluff Formation of Livingston Island (Figure 1) is also included for comparison, for which Hervé et al. (2006) interpreted a Jurassic depositional age and determined it was not part of the Trinity Peninsula Group succession. The Miers Bluff Formation also has a prominent Permian peak at c. 270 Ma, but is also characterized by a prominent c. 170 Ma peak reflecting its younger depositional age (Figure 9).

6.1.6. Patagonia

The Carboniferous—Triassic metasedimentary successions of the northern Antarctic Peninsula are considered correlatives, at least in part, to the Duque de York Complex metaturbidites (Sepúlveda et al., 2010). The Duque de York Complex of southern Patagonia forms part of a series of low-grade metamorphic accretionary complexes (Madre de Dios Complex). Akin to the Trinity Peninsula Group of northern Graham Land, the Duque de York Complex has a dominant Permian age of source material and presumed depositional age (Barbeau et al., 2010; Castillo et al., 2015, 2016; Fanning et al., 2011).

6.2. LeMay Group: Interpretation

Several authors (e.g., Tranter, 1988; Vaughan & Storey, 2000; Willan, 2003) have all suggested that the LeMay Group accretionary complex of Alexander Island was unlikely to have developed autochthonously. Vaughan and Storey (2000) interpreted the tectonic history of the Antarctic Peninsula as an amalgamation of autochthonous, para-autochthonous and allochthonous terranes, with Alexander Island forming the western domain (Figure 1) and was interpreted to be far-traveled. Tranter (1988) and Willan (2003) presented petrographic and geochemical evidence that suggested the LeMay Group may have had an exotic sediment source as it was not consistent with the proximal arc. Both Tranter (1988) and Willan (2003) presented petrographic data and facies analysis indicating at least two different components to the LeMay Group, one more akin to the Fossil Bluff Group and the other very similar to the source of the Trinity Peninsula Group. The age and Lu-Hf isotope analysis presented here, combined with existing field and petrographic data, permit a more complete evaluation of the provenance of the LeMay Group accretionary complex and the role of allochthonous/para-autochthonous terranes in the tectonic history of the Antarctic Peninsula.

The four separate groups identified within the LeMay Group are geographically separated, although some spatial overlap occurs between Groups 1 and 2. Group 1 is identified from the main succession of the LeMay Group exposed in the LeMay Range, Walton Mountains, Atoll Nunataks, Mount Umbriel and Hornpipe Heights (Figure 3). The samples are from sandstone-shale sequences that in the LeMay Range and Walton Mountains are adjacent to a mélange belt (Tranter, 1991) associated with accreted oceanic material (Figure 3). Group 1 lithologies are characterized by detrital zircon age profiles with prominent Permian (c. 255 Ma) and Cambrian (c. 530 Ma) peaks, plus a minor Ordovician (c. 470 Ma) peak. They have a broad spread of Neo- to Mesoproterozoic ages, but a low number of ages >1,200 Ma (Table S2). Multi-dimensional scaling (MDS) plots (Figure 10) are used here to evaluate potential correlative units from the West Gondwana margin and to identify those samples that may share a common source. Figure 10a illustrates that the LeMay Group (Group 1) has a close similarity to the Permian quartz-rich sandstones from southern Palmer Land at Erewhon Nunatak and Mount Peterson (Figure 1), but also to components of the Scotia Metamorphic Complex (e.g., Bruce Bank, Coronation Island) and the Trinity Peninsula Group. The c. 530 Ma peak characteristic of Group 1 is less prominent in the Trinity Peninsula Group or Duque de York Complex (Figure 9), but is a significant feature of the Scotia Metamorphic Complex from the South Scotia Ridge (Figure 9). However, by examining only the <300 Ma age population a subtly different picture emerges (Figure 10b). The restricted zircon age range yields more valuable provenance information than examining the entire detrital age population (e.g., Andersen, 2005), particularly as the Gondwana margin is characterized by multi-phase recycling of Ordovician and Cambrian zircons (e.g., Andersen et al., 2018). Group 1 still exhibit a close similarity to the quartz-rich sandstones from Erewhon Nunatak and Mount Peterson (Figure 1), but also show a close similarity to Group 2 indicating a similar or partially overlapping Permian signal (Figure 10b). Other units also show a much closer relationship by investigating the <300 Ma

population. The Trinity Peninsula Group of the northern Antarctic Peninsula and the Duque de York Complex of southern Patagonia exhibit an overlap when only the Permian signal is examined (Figure 10b).

The addition of Lu-Hf isotope data to the MDS plots (Figure 11 and Table S6) permits an additional level of information to examine provenance similarity. Only a subset of the samples used in the age-only MDS analysis (Figure 10) have Lu-Hf isotope data available (Figure 6), but there is sufficient data coverage to still permit interpretations across large parts of the margin, although the absence of Lu-Hf data from the Scotia Metamorphic Complex is unfortunate. The Hf data are plotted as model ages to differentiate between εHf values that are the same for zircon grains of different ages (see Supporting Information S1). The Group 1 field exhibits no clustering with any of the other units in the combined age-Hf plot (Figure 11a), although the nearest-neighbor relationship with the Erewhon Beds and the lower Latady Group may indicate a similar source. However, by examining only the zircon grains with ages <300 Ma to better correlate the Jurassic and Permian source areas (Figure 11b) it shows that Group 1 lithologies exhibit clustering with the Duque de York Complex of southern Patagonia and the lower Latady Group sedimentary succession. This correlation is also evident in Figure 6 where the εHf distribution of the Duque de York Complex and Trinity Peninsula Group exhibit a very similar distribution to Groups 1 and 2 of the LeMay Group with Group 1 and the Duque de York Complex forming a slightly younger population with more negative εHf_i values.

The Group 2 succession of the LeMay Group is identified from the Douglas Range and, akin to Group 1, is dominated by a Permian peak at c. 260 Ma, but lacks almost any Cambrian population that is a major characteristic of Group 1. The detrital zircon MDS (Figure 10a) and age spectra plot (Figure 9) illustrate a significant disparity between LeMay Groups 1 and 2, but by excluding the Cambrian age population (Figure 10b) a nearest neighbor relationship is evident, albeit with a slight age difference. Group 2 exhibits a nearest neighbor elationship to the quartz-rich sandstones of Mount Peterson and Erewhon Nunatak, as well as components of the Scotia Metamorphic Complex when examining the <300 Ma age population (Figure 10b). When the available εHf data is considered for <300 Ma (Figure 11b), the Group 2 succession has a nearest neighbor relationship to the metasedimentary succession of the Trinity Peninsula Group and a far more remote similarity to the sandstones of Mount Peterson and Erewhon Beds. These units lie much further along the Hf vector (Figure 11b) despite a close age relationship (minor shift along the age vector). Also, by examining the age and Hf data for the <300 Ma population a clustering relationship between Groups 1 and 2 of the LeMay Group is now evident.

The Group 3 succession of the LeMay Group is only identified from Charcot Island to the west of Alexander Island (Figure 3). The Charcot Island sequence has a very different age profile to Groups 1 and 2 of the LeMay Group succession of central Alexander Island. Group 3 lacks any Permian signal that is dominant in Groups 1 and 2, but instead is characterized by a minor mid-Cretaceous peak, a prominent Early—Middle Jurassic peak, a minor Cambrian peak and a broad spread of Neoproterozoic ages (Figure 5). Also, the number of ages >1,200 Ma is approximately 10% of the total analyzed, compared to typically <2% for Groups 1 and 2 (Figure 4). The MDS plot which incorporates all ages (Figure 10a) illustrates the units with the nearest neighbor relationship to Group 3 are components of the Latady Group sedimentary succession, the lower part of the Mount Hill Formation and also metasedimentary rocks of the North Scotia Ridge and components of Bruce Bank (Figure 2). When the <300 Ma age population is considered (Figure 10b) in isolation, which is of greater significance for determining source and shared provenance, the Group 3 succession exhibits clustering to the Latady Group and Bruce Bank (DR.225.28). This nearest neighbor association to the Latady Group is also supported by the combined age and Hf MDS plot (Figure 11), but with slightly greater disparity than the age-only MDS plot (Figure 10b). The εHf data for Group 3 show a discrete field for the Early Jurassic zircons (−7 to −12; Figure 6 and Table 1) which closely corresponds to the lower part of the Latady Group and within the range defined by the Early Jurassic Mount Poster Formation (εHf: −2 to −15; BAS unpublished data, Table 1). A potential correlation with the Thurston Island crustal block is also considered, although it does not preserve any sedimentary successions (Riley et al., 2017). Thurston island is characterized by Early Jurassic volcanic rocks with εHf in the range −3 to −12 (Riley et al., 2017) and were considered correlatives of the Mount Poster Formation, as well as mid-Cretaceous (c. 108 Ma) magmatism (εHf: −2 to −10; Riley et al., 2017). Thurston Island also preserves Carboniferous and Triassic magmatism (Riley et al., 2017) which are minor components of the Group 3 age profile (Figure 5). Simões Pereira et al. (2018) investigated shallow (<25 m) offshore sediment cores adjacent to Thurston Island (Figure 2) and detrital biotite and hornblende age populations show prominent mid-Cretaceous (c. 110 Ma) and Middle Jurassic (c. 170 Ma) age peaks. They exhibit clustering with Group 3 in Figure 10b, but with a more significant mid-Cretaceous component.

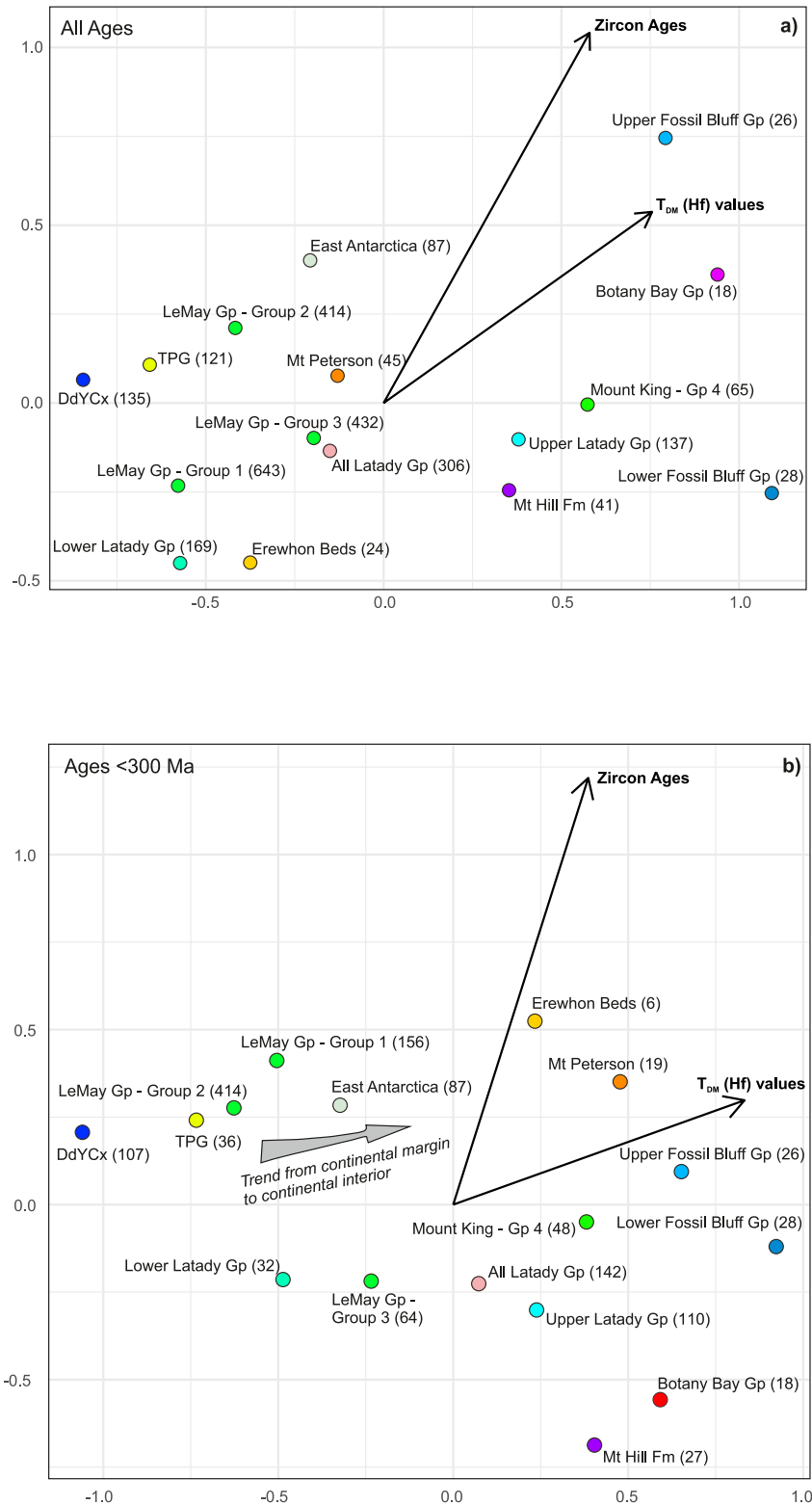**Figure 11.** Combined age-Hf MDS plot for (a) all ages and (b) ages <300 Ma. Data sources for age data as for Figure 8 and Lu-Hf data from Figure 6. Hf data are plotted as Hf depleted mantle model ages. The vectors indicate that variation along that broad trend reflects either age or Hf differences. Numbers in parentheses are number of analyses. TPG: Trinity Peninsula Group; DdYCx: Duque de York Complex.

Table 1
Accretionary Complexes Age Summary

Unit	Approx age peaks (Ma)	εHf range
Le May Group (Group 1)	255	0 to −6
	530	2 to −7
Le May Group (Group 2)	262	2 to −4
Le May Group (Group 3)	121	−2 to −10
	185	−7 to −12
Le May Group (Group 4)	225	0 to −10
Trinity Peninsula Group	265	3 to −5
	470	2 to −5
Duque de York Complex	262	0 to −8
Latady Group	150	3 to −5
	185	−2 to −10
	220	−5 to −9
Fossil Bluff Group	110	0 to −8
	145	1 to 6
	180	2 to −4
Scotia Metamorphic Complex	260	No data
	530	No data
Erewhon-Mount Peterson	260	5 to −7
Mount Poster Formation	185	−2 to −15

The mid-Cretaceous minor age peak evident in the Group 3 lithologies from Charcot Island is likely to be related to a widespread magmatic event of West Gondwana (e.g., Decker et al., 2017; Riley et al., 2018). The mid-Cretaceous zircons from the Group 3 succession have a range in εHf from −2 to −5, with two grains at c. −10 (Figure 6a). The Lassiter Coast intrusive suite of Palmer Land (Figure 12d) have εHf values of −7 (Riley, Flowerdew, Burton-Johnson, et al., 2020), whilst mid-Cretaceous granitoids from Thurston Island have εHf values in the range 0 to −10 (Riley et al., 2017). Cretaceous volcanic rocks of northwest Palmer Land have εHf in the range 0 to −3 (Riley, Flowerdew, Burton-Johnson, et al., 2020). Mid-Cretaceous volcanism has also been identified from central Alexander Island (Gannon Nunatak; Figure 4v) where a volcanic tuff has an emplacement age of 117.5 ± 1.0 Ma (Figure S1 in Supporting Information S1) and represents a potential proximal source for the mid-Cretaceous component of the Group 3 (Charcot Island) age profile. Mid-Cretaceous volcanic rocks may have formed a more extensive cover across Alexander Island, but was potentially removed during Cenozoic rapid uplift and erosion (Twinn et al., 2022). Another key feature of Group 3 is the broad spread of ages >500 Ma which is also a prominent characteristic of the Latady Group (Figure 9) and Bruce Bank (DR.225.28).

LeMay Group (Group 4) forms another distinct sequence only exposed at Mount King (Figure 3), although there is uncertainty regarding its exact relationship to the broader LeMay Group succession (Kelly et al., 2001). The age profile for the analyzed sandstone from Mount King (Figure 4u) has a prominent Triassic peak at c. 225 Ma, but lacks the Permian peak characteristic of Groups 1 and 2, and akin to Group 3, the Group 4 sandstone is also characterized by a significant contribution of Early Jurassic zircons. The MDS plots indicate that the Group 4 succession at Mount King exhibits no clustering in the <300 Ma plot (Figure 10b), but its nearest neighbor is the Torlesse Supergroup of the eastern domain of New Zealand in the all-ages plot (Figure 10a). Using the combined age and Hf MDS plot (Figure 11) for both the <300 Ma and all ages, it is evident that the Group 4 sandstone from Mount King is quite distinct to all the other units of the wider LeMay Group. Kelly et al. (2001) also noted that the Mount King beds may not correlate with the main succession of the LeMay Group. Based on the marine macrofauna assemblage from the calcareous mudstones at Mount King, Kelly et al. (2001) interpreted an Early Carboniferous—Permian age range that is not consistent with the detrital zircon age profile presented here (Figure 4u), which is characterized by Triassic and Early Jurassic zircons. The εHf data from Mount King (Group 4) show that the Early Jurassic zircons form a separate population (Figure 6a) to the Early Jurassic zircon population from Charcot Island (Group 3). The Mount King (Group 4) Early Jurassic zircons have an εHf range of −1 to −5 and are marginally younger (<180 Ma) than those from Charcot Island (Group 3) and are closer in age and composition to the Early—Middle Jurassic silicic volcanic rocks of the northern Antarctic Peninsula and Patagonia (Pankhurst et al., 2000; BAS unpublished data). The Triassic—Jurassic component of Group 4 also overlap to a large degree with the Early Mesozoic component of the upper Latady Group, which is also confirmed by the statistical analysis (Figures 9 and 10). The Triassic age population for Group 4 has an εHf range from 0 to −10 and overlaps with a small number of Triassic zircons from Group 3. Evidence for a Triassic magmatic arc across the Antarctic Peninsula and Patagonia have been presented by Navarrete et al. (2019), Bastias et al. (2020), and Riley, Flowerdew, Millar, and Whitehouse (2020) and indicates the presence of a proximal Triassic source.

6.3. Depositional Age

In the absence of a diagnostic fossil assemblage or directly dateable volcanic layers, detrital geochronology is often the only method to estimate the depositional age of siliciclastic rocks. Detrital zircon U–Pb geochronology in particular has become a popular technique to obtain maximum depositional ages, but there is little consistency in the estimation algorithms used. We follow the approach of Vermeesch (2021) to calculate the maximum likelihood age of deposition (MLA) for the LeMay Group samples analyzed in this study (see Section S1.4 in Supporting Information S1). The results are presented in Figure S2 in Supporting Information S1 using radial
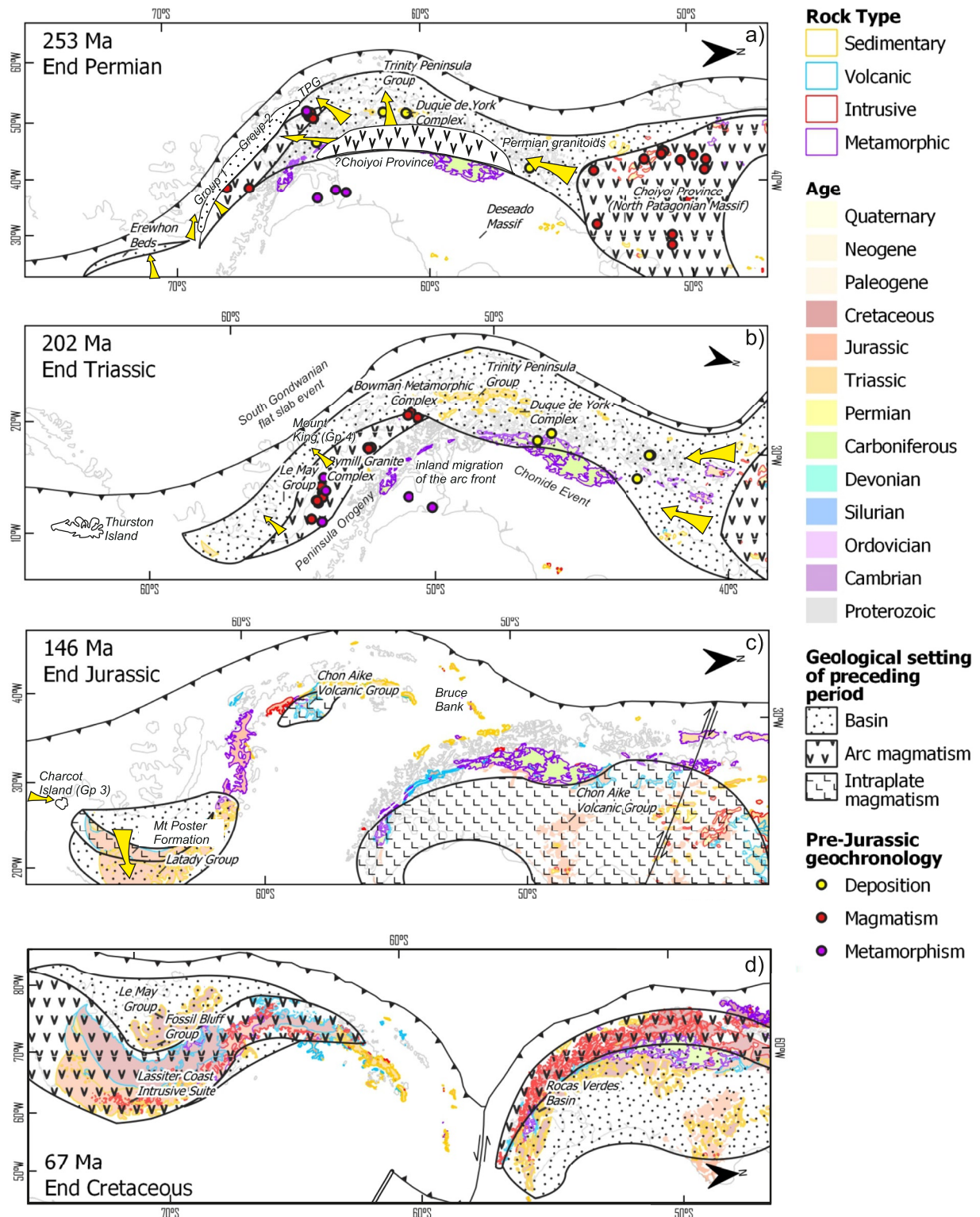
Figure 12. Kinematic GPlates reconstruction for the Late Paleozoic–Early Mesozoic Gondwana margin illustrating the accretionary complexes of the LeMay Group, Scotia Metamorphic Complex, Trinity Peninsula Group and Duque de York, and the Triassic extent of the Peninsula Orogeny-Chonide Event. TPG: Trinity Peninsula Group. Adapted from Riley et al. (2023). Yellow arrows depict potential sediment transport.

plots to derive the MLA, but prior knowledge of the geological setting and field relationships are essential to fully understand the derived MLA.

Group 1 lithologies yield MLAs in the range 263–232 Ma (Figure S2 in Supporting Information S1), akin to those derived from Group 2 (263–251 Ma) strongly suggesting a Late Permian/Early Triassic depositional age akin to that suggested for the main succession of the Trinity Peninsula Group (e.g., Castillo et al., 2016). One Group 1 sample from Richter Peaks (Figure 3) has a prominent Late Jurassic (c. 148 Ma) age peak alongside the Permian and Cambrian peaks typical of Group 1 and this lithology yields an MLA of c. 140 Ma.

The Group 3 lithologies from Charcot Island show a tight cluster of MLAs at c. 110 Ma, with one sample (KG.4832.25) having an older age of c. 129 Ma (Figure S2 in Supporting Information S1), but still broadly consistent with a likely depositional age during the mid-Cretaceous.

The single sample from Mount King (Group 4) has an MLA of c. 178 Ma and supports the field observations and lithology descriptions that Mount King is distinct to the main LeMay Group succession.

6.4. Tectonic Implications and Accretion

Several authors have attempted to correlate West Gondwana accretionary complexes through Patagonia, West Antarctica and New Zealand (e.g., Nelson & Cottle, 2019; Figure 8), but robust interpretations about the tectonic setting are difficult without more reliable provenance information and likely depositional age.

The analysis of the LeMay Group accretionary complex and comparison with sedimentary successions from along the margin presented here permit an improved understanding of the depositional and tectonic history of the West Gondwana margin during the Late Paleozoic—Early Mesozoic (Figure 12). We favor a Late Permian—Triassic depositional age (Section 6.3) for the main sequences of the LeMay Group (Groups 1 and 2) exposed in central Alexander Island, akin to the accretionary complexes of the northern Antarctic Peninsula (Trinity Peninsula Group) and Patagonia (Duque de York Complex). All these successions are dominated by sediment input from a penecontemporaneous volcanic/volcaniclastic source emplaced in the interval 265–250 Ma (Figure 12a; Choiyoi Province; Gianni & Navarrete, 2022) or Permian granitoids (Castillo et al., 2017). However, one key difference is that the secondary age peak of the Trinity Peninsula Group (and Duque de York Complex) is Ordovician (c. 470 Ma), aligned to a source derived from the extensive Famatinian magmatic belt (Castillo et al., 2017). Whereas the LeMay Group has a secondary age peak that is Cambrian in age and likely reflects input from a recycled East Antarctic/Gondwana source. This suggests that although the LeMay Group and Trinity Peninsula Group were broadly contiguous, their sedimentary input was distinct, although both are dominated by likely input from the widespread Permian Choiyoi volcanic province. The Group 2 succession of the LeMay Range may mark the transition zone between Group 1 and the Trinity Peninsula Group (Figure 12), as the Cambrian age peak typical of Group 1 is absent in Group 2, but is instead characterized by a minor Ordovician peak (c. 470 Ma; Figure 4k), more akin to the Trinity Peninsula Group.

Willner et al. (2009) investigated the metamorphic history of the Duque de York accretionary prism as part of the Madre de Dios metamorphic complex and assigned an accretion age of c. 233 Ma. They dated (^{40}Ar/^{39}Ar) white mica that they interpreted was the result of deformation associated with accretion. A similar age was reported from the Cape Legoupil Formation of the Trinity Peninsula Group (Trouw et al., 1997) who determined a Rb-Sr metamorphic age of 232 + 5 Ma, which they also attributed to possible accretion. In the South Orkney Islands, chert horizons have been recognized from the Scotia Metamorphic accretionary complex and assigned a Triassic age (Holdsworth & Nell, 1992), consistent with other components of the Gondwana margin accretion events and in agreement with the findings of Flowerdew et al. (2007) who suggested an accretion age of c. 190 Ma from the South Orkney Islands.

White mica from sandstone at Grikurov Ridge (Group 1) was analyzed as part of this study and yielded ages in the range 267–232 Ma, which largely reflects the likely depositional age, but the younger white mica ages, which map the later foliation may reflect the age of accretion. Triassic accretion may be related to the final phase of the Gondwanide Orogeny or the more localized Late Triassic Peninsula/Chonide orogenies of the Antarctic Peninsula-Patagonia related to flat-slab subduction (e.g., Navarrete et al., 2019; Riley, Flowerdew, Millar, & Whitehouse, 2020). Although the Gondwanide Orogeny is recognised from the North Patagonian Massif (Gregori et al., 2016) and parts of West Antarctica (Curtis & Storey, 1996), Storey et al. (1987) considered the Mesozoic

deformation in the Antarctic Peninsula was too young to represent an extension of the main Gondwanide Orogeny and coined the term, the "Peninsula Orogeny" to define an episode of Late Triassic—Early Jurassic transtension. Gregori et al. (2016) have determined two phases of Gondwanide deformation (Chonide Event) in the North Patagonian Massif commencing at 224 ± 5 Ma whilst Riley, Flowerdew, Millar, and Whitehouse (2020) recorded an age of c. 221 Ma for deformation in northwest Palmer Land, which they attributed to the Peninsula Orogeny.

The Group 3 succession at Charcot Island is entirely distinct to the Late Permian—Early Triassic successions of Groups 1 and 2 of the LeMay Group. A mid-Cretaceous depositional age (Section 6.3) is favored for the sequences on Charcot Island with a source predominantly derived from Early—Middle Jurassic and mid-Cretaceous lithologies. The Early Jurassic source is closely aligned to the Mount Poster Formation (c. 183 Ma; Hunter et al., 2006) of southern Palmer Land that also sourced the marine sandstones and mudstone of the Latady Group of (Figure 1). Early Jurassic volcanic rocks which have been correlated to the Mount Poster Formation are also exposed in the adjacent Thurston Island crustal block (Riley et al., 2017; Figure 2) and eroded components are likely to extend offshore into the Amundsen Sea (Simões Pereira et al., 2018).

The mid-Cretaceous age signal in Group 3 could be related to the local expression of silicic volcanism exposed at Gannon Nunatak (Figure 3), but could also be related to the relatively proximal and extensive mid-Cretaceous Lassiter Coast intrusive suite of Palmer Land (Riley, Flowerdew, Burton-Johnson, et al., 2020; Riley et al., 2018) and its correlatives exposed in Thurston Island (Riley et al., 2017). The greater proportion of ages >1,200 Ma identified in Group 3 (>10%) relative to Groups 1 and 2 may reflect the close proximity of a translated Charcot Island to the Haag Nunataks crustal block (Riley, Flowerdew, Pankhurst, et al., 2020).

The dredged samples from Bruce Bank (Figure 2a), a submerged crustal block of the South Scotia Ridge, are of direct significance to the LeMay Group accretionary complex. Bruce Bank forms part of the widespread Scotia Metamorphic Complex and metasedimentary rocks along its southern margin have a very similar detrital zircon age profile to Group 1 of the LeMay Group with peaks at c. 262 Ma and c. 520 Ma (Figure 9; Riley, Carter, et al., 2022; Riley, Burton-Johnson, et al., 2022). However a sample from the eastern margin of Bruce Bank (DR.225.28) has a very distinct profile with detrital zircon age peaks at c. 128 Ma and c. 185 Ma (Figure 9), strikingly similar to the Group 3 lithologies of Charcot Island and with a similar spatial relationship. Riley, Carter, et al. (2022) and Riley, Burton-Johnson, et al. (2022) interpreted that Bruce Bank, along with the South Orkney microcontinent, formed part of the Antarctic Plate prior to translation to form the South Scotia Ridge. In the mid-Cretaceous, Bruce Bank would have been located adjacent to the Gondwana margin in continuity with the other accretionary complexes (Figures 12b and 12c).

A clear temporal association between Group 3 (Charcot Island), the Latady Group/Mount Poster Formation, Thurston Island and Bruce Bank indicates that Charcot Island (and Bruce Bank) may have undergone some degree of translation as para-autochthonous crustal blocks. Transcurrent-transform motion is commonplace along oblique margins and this often leads to the translation of allochthonous terranes (e.g., Umhoefer & Dorsey, 1997). The tectonic setting was certainly favorable for the translation of allochthonous terranes in the late Mesozoic and Gohl et al. (1997) noted that relative motion between the Antarctic-Bellingshausen Plate and the Phoenix Plate could have developed a transcurrent plate boundary to accommodate the relative motion between the Antarctic-Bellingshausen Plate and the southward migrating and subducting Phoenix Plate.

Another possibility is that there is a more significant outboard sedimentary succession with a source characterized by mid-Cretaceous and Early—Middle Jurassic age profiles. The identification by Simões Pereira et al. (2018) of offshore sediments dominated by a detrital source with c. 110 Ma and c. 170 Ma ages lends support to a more extensive outboard unit extending from the Amundsen Sea, adjacent to Thurston Island. Whilst this does not rule out an allochthonous origin for the Charcot Island crustal block, it could equally have developed para-autochthonously as part of this outboard sedimentary succession.

Accretion of Charcot Island and components of Bruce Bank must have developed post-110 Ma (likely depositional age) and may align with the accretion event suggested by Holdsworth and Nell (1992) at c. 90 Ma based on *Radiolaria* of Tethyan origin from accreted chert and associated ocean floor material. We favor that the accretion of the thrust-bound mélange belts in central Alexander Island (Figure 3) are likely to be associated with the accretion of the Charcot Island block at <90 Ma. Larter et al. (2002) determined that the subduction of a microplate (termed the Charcot Plate) stalled at c. 83 Ma and became coupled to the Antarctic Plate, which may also be correlated to Late Cretaceous accretion. Apatite fission track ages from Storey et al. (1996) for Charcot Island are

between 46 and 54 Ma and are similar to other LeMay Group units from the east, indicating a shared history by the Early Cenozoic. Apatite fission track data from the Lataday Group (Twinn et al., 2022) are comparable to the Storey et al. (1996) data from Charcot Island and are consistent with a regional exhumation event spanning the latest Cretaceous/early Cenozoic related to changes in plate convergence rate as discussed in Twinn et al. (2022) and also highlighted by Larter et al. (2002).

The Group 4 sequence exposed at Mount King is anomalous with respect to the other components of the LeMay Group and also the adjacent Fossil Bluff Group of eastern Alexander Island. The Carboniferous—Permian depositional age determined from the macrofauna assemblage reported by Kelly et al. (2001) is not consistent with the detrital zircon data presented here, which has a prominent Early Jurassic component. The fossil assemblage from Mount King is not diagnostic and so Early Jurassic deposition for Group 4 is likely following the accretion of Groups 1 and 2, with a primary contribution from the adjacent Triassic arc of northwest Palmer Land (Riley, Flowerdew, Millar, & Whitehouse, 2020).

7. Summary

1. The LeMay Group accretionary complex of Alexander Island in the southern Antarctic Peninsula has been subdivided into four separate groups based on detrital zircon U-Pb age spectra and Lu-Hf isotope provenance analysis. It is interpreted to be related to the accretionary complexes of the Trinity Peninsula Group (northern Antarctic Peninsula) and the Madre de Dios complexes of southern Patagonia, while there are also potential outboard connections to the neighboring Thurston Island crustal block and the Scotia Metamorphic Complex.

2. Groups 1 and 2 of the LeMay Group have a likely depositional age of c. 255 Ma and are closely aligned to the depositional histories of the Trinity Peninsula Group and the Duque de York Complex of Patagonia. We favor an autochthonous or para-autochthonous origin for the turbidite succession. Accretion developed at c. 233 Ma along large parts of the West Gondwana margin and may be related to the localized Peninsula Orogeny during a period of flat-slab subduction. Post-accretion deposition developed across parts of the LeMay Group (e.g., Richter Peaks) and may be akin to the Miers Bluff Formation succession on Livingston Island of the South Shetland Islands.

3. Group 3 is restricted to Charcot Island and is a distinct lithological unit to Groups 1 and 2, with a likely depositional age of ~110 Ma. Group 3 has a source derived from lithologies akin to the Early Jurassic Mount Poster Formation of southern Palmer Land and mid-Cretaceous magmatism widespread across the southern Antarctic Peninsula. Group 3 has close similarities to components of the South Scotia Ridge at Bruce Bank, which forms part of the Scotia Metamorphic Complex and also to the Thurston Island-Amundsen Sea region, where offshore sedimentary units dominated by Early—Middle Jurassic and mid-Cretaceous age profiles are extensive. We favor a para-autochthonous origin for the Group 3 Charcot Island succession with accretion developing after 90 Ma associated with thrust slices of oceanic material in the central mélange belts of Alexander Island. This event is likely to be coincident with the uplift of blueschist-facies lithologies from Smith Island (Figure 1; Scotia Metamorphic Complex; McCarron & Larter, 1998). An outboard origin is most likely, but translation from close to the Thurston Island crustal block is consistent with the plate reorganisation developing during the Late Cretaceous.

4. Group 4 (Mount King) also forms a separate lithological unit distinct from the LeMay and Fossil Bluff groups. We favor a post-accretion depositional age (Early Jurassic) and do not support a Carboniferous lithostratigraphical age suggested by the non-diagnostic macrofauna assemblage.

5. The primary source for Groups 1 and 2 of the LeMay Group are closely related to the emplacement of the widespread Choiyoi magmatic event during the Permian as part of slab window events. The extent of the Choiyoi province is likely to continue into the Antarctic Peninsula but with the volcanic record only preserved in offshore basins.

Data Availability Statement

The data that support this research are all available as Supporting Information files linked to this article. Full datasets are also hosted at the British Antarctic Survey's Polar Data Centre via the following link (https://doi.org/10.5285/C0C56E6D-D13B-4480-BBD3-CD613AB57B33).

References

Andersen, T. (2005). Detrital zircons as tracers of sedimentary provenance: Limiting conditions from statistics and numerical simulation. *Chemical Geology*, *216*(3–4), 249–270. https://doi.org/10.1016/j.chemgeo.2004.11.013

Andersen, T., Elburg, M. A., van Niekerk, H. S., & Ueckermann, H. (2018). Successive sedimentary recycling regimes in southwestern Gondwana: Evidence from detrital zircons in Neoproterozoic to Cambrian sedimentary rocks in southern Africa. *Earth-Science Reviews*, *181*, 43–60. https://doi.org/10.1016/j.earscirev.2018.04.001

Barbeau, D. L., Davis, J. T., Murray, K. E., Valencia, V., Gehrels, G. E., Zahid, K. M., & Gombosi, D. J. (2010). Detrital-zircon geochronology of the metasedimentary rocks of north-western Graham Land. *Antarctic Science*, *22*(01), 65–78. https://doi.org/10.1017/s095410200999054x

Bastias, J., Calderon, M., Israel, L., Hervé, F., Spikings, R., Pankhurst, R., et al. (2019). The Byers Basin: Jurassic-Cretaceous tectonic and depositional evolution of the forearc deposits of the South Shetland Islands and its implications for the northern Antarctic Peninsula. *International Geology Review*, *62*(11), 1467–1484. https://doi.org/10.1080/00206814.2019.1655669

Bastias, J., Spikings, R., Riley, T., Ulianov, A., Grunow, A., Chiaradia, M., & Hervé, F. (2021). A revised interpretation of the Chon Aike magmatic province: Active margin origin and implications for the opening of the Weddell Sea. *Lithos*, *386–387*, 106013. https://doi.org/10.1016/j.lithos.2021.106013

Bastias, J., Spikings, R., Ulianov, A., Riley, T., Burton-Johnson, A., Chiaradia, M., et al. (2020). The Gondwanan margin in west Antarctica: Insights from late Triassic magmatism of the Antarctic Peninsula. *Gondwana Research*, *81*, 1–20. https://doi.org/10.1016/j.gr.2019.10.018

Birkenmajer, K. (1992). Trinity Peninsula group (Permo-Triassic?) at Hope Bay, Antarctic Peninsula. *Polish Polar Research*, *13*, 215–240.

Bouvier, A., Vervoort, J. D., & Patchett, P. J. (2008). The Lu–Hf and Sm–Nd isotopic composition of CHUR: Constraints from unequilibrated chondrites and implications for the bulk composition of terrestrial planets. *Earth and Planetary Science Letters*, *273*(1), 8–57. https://doi.org/10.1016/j.epsl.2008.06.010

Bradshaw, J. D., Vaughan, A. P. M., Millar, I. L., Flowerdew, M. J., Trouw, R. A. J., Fanning, C. M., & Whitehouse, M. J. (2012). Permo-Carboniferous conglomerates in the Trinity Peninsula group at view point, Antarctic Peninsula: Sedimentology, geochronology and isotope evidence for provenance and tectonic setting in Gondwana. *Geological Magazine*, *149*(4), 626–644. https://doi.org/10.1017/s001675681100080x

Burn, R. W. (1984). *The geology of the LeMay Group, Alexander island. British Antarctic survey scientific reports, 109*. British Antarctic Survey.

Burton-Johnson, A., & Riley, T. R. (2015). Autochthonous vs. accreted terrane development of continental margins: A new in situ tectonic history of the Antarctic Peninsula. *Journal of the Geological Society*, *172*(6), 822–835. https://doi.org/10.1144/jgs2014-110

Butterworth, P. J., Crame, J. A., Howlett, P. J., & Macdonald, D. I. M. (1988). Lithostratigraphy of upper jurassic-lower Cretaceous strata of eastern Alexander island. *Cretaceous Research*, *9*(3), 249–264. https://doi.org/10.1016/0195-6671(88)90020-1

Carter, A., Riley, T. R., Hillenbrand, C.-D., & Rittner, M. (2017). Evidence for an extensive Antarctic ice sheet during the Late Eocene. *Earth and Planetary Science Letters*, *458*, 49–57. https://doi.org/10.1016/j.epsl.2016.10.045

Castillo, P., Fanning, C. M., Fernandez, R., Poblete, F., & Hervé, F. (2017). Provenance and age constraints of Palaeozoic siliciclastic rocks from the Ellsworth Mountains in West Antarctica, as determined by detrital zircon geochronology. *The Geological Society of America Bulletin*, *129*, 1568–1584.

Castillo, P., Fanning, C. M., Hervé, F., & Lacassie, J. P. (2016). Characterisation and tracing of Permian magmatism in the south-western segment of the Gondwana margin: U-Pb age, Lu-Hf and O isotopic compositions of detrital zircons from metasedimentary complexes of northern Antarctic Peninsula and western Patagonia. *Gondwana Research*, *36*, 1–13. https://doi.org/10.1016/j.gr.2015.07.014

Castillo, P., Lacassie, J. P., Augustsson, C., & Hervé, F. (2015). Petrography and geochemistry of the Carboniferous-Triassic Trinity Peninsula group, west Antarctica: Implications for provenance and tectonic setting. *Geological Magazine*, *152*(4), 575–588. https://doi.org/10.1017/s0016756814000454

Cawood, P. A. (2005). Terra Australis orogen: Rodinia breakup and development of the Pacific and Iapetus margins of Gondwana during the Neoproterozoic and Palaeozoic. *Earth-Science Reviews*, *69*(3–4), 249–279. https://doi.org/10.1016/j.earscirev.2004.09.001

Curtis, M. L., & Storey, B. C. (1996). A review of geological constraints on the pre-break-up position of the Ellsworth Mountains within Gondwana: Implications for Weddell Sea evolution, In B. C. Storey, et al. (Eds.). In *Weddell Sea tectonics and Gondwana break-up* (Vol. 108, pp. 11–30). Geological Society, Special Publications.

Dalziel, I. W. D., Lawver, L., Norton, I. O., & Gahagan, L. M. (2013). The Scotia arc: Genesis, evolution, global significance. *Annual Review of Earth and Planetary Sciences*, *41*(1), 767–793. https://doi.org/10.1146/annurev-earth-050212-124155

Decker, M., Schwartz, J. J., Stowell, H. H., Klepeis, K. A., Tulloch, A. J., Kitajima, K., et al. (2017). Slab-triggered arc flare-up in the Cretaceous Median Batholith and the growth of lower arc crust, Fiordland, New Zealand. *Journal of Petrology*, *58*(6), 1145–1171. https://doi.org/10.1093/petrology/egx049

Doubleday, P. A., Leat, P. T., Alabaster, T., Nell, P. A. R., & Tranter, T. H. (1994). Allochthonous oceanic basalts within the Mesozoic accretionary complex of Alexander island, Antarctica: Remnants of proto-Pacific oceanic crust. *Journal of the Geological Society*, *151*(1), 65–78. https://doi.org/10.1144/gsjgs.151.1.0065

Doubleday, P. A., Macdonald, D. I. M., & Nell, P. A. R. (1993). Sedimentology and structure of the trench-slope to fore-arc basin transition in the Mesozoic of Alexander Island, Antarctica. *Geological Magazine*, *130*(6), 737–754. https://doi.org/10.1017/s0016756800023128

Eagles, G., & Eisermann, H. (2020). The Skytrain plate and tectonic evolution of southwest Gondwana since Jurassic times. *Scientific Reports*, *10*(1), 19994. https://doi.org/10.1038/s41598-020-77070-6

Edwards, C. W. (1980). The geology of central and eastern Alexander Island. Ph.D. thesis (p. 228). University of Birmingham.

Elliot, D. H., Fanning, C. M., & Laudon, T. S. (2016). The Gondwana plate margin in the Weddell Sea sector: Zircon geochronology of upper Palaeozoic (mainly Permian) strata from the Ellsworth Mountains and eastern Ellsworth Land, Antarctica. *Gondwana Research*, *29*(1), 234–247. https://doi.org/10.1016/j.gr.2014.12.001

Fanning, C. M., Hervé, F., Pankhurst, R. J., Rapela, C. W., Kleiman, L. E., Yaxley, G. M., & Castillo, P. (2011). Lu–Hf isotope evidence for the provenance of Permian detritus in accretionary complexes of western Patagonia and the northern Antarctic Peninsula region. *Journal of South American Earth Sciences*, *32*(4), 485–496. https://doi.org/10.1016/j.jsames.2011.03.007

Flowerdew, M. J., Daly, J. S., & Riley, T. R. (2007). New Rb-Sr mineral ages temporally link plume events with accretion at the margin of Gondwana USGS Open- File Report 2007-1047, Short Research Paper 012. In A. K. Cooper, C. R. Raymond et al. (Eds.), *A keystone in a changing world—Online proceedings of the 10th ISAES* (pp. 4). https://doi.org/10.3133/of2007-1047.srp012

Flowerdew, M. J., Riley, T. R., & Haselwimmer, C. E. (2011). *Geological map of the South Orkney Islands (1:150 000 scale): BAS GEOMAP 2 Series, sheet 3*. British Antarctic Survey.

Tectonics

10.1029/2022TC007578

Gao, L., Pei, J. L., Zhao, Y., Yang, Z. Y., Riley, T. R., Liu, X. C., et al. (2021). New paleomagnetic constraints on the cretaceous tectonic framework of the Antarctic Peninsula. *Journal of Geophysical Research: Solid Earth*, *126*(11), 1–17. https://doi.org/10.1029/2021jb022503

Gianni, G. M., & Navarrete, C. R. (2022). Catastrophic slab loss in southwestern Pangea preserved in the mantle and igneous record. *Nature Communications*, *13*(1), 698. https://doi.org/10.1038/s41467-022-28290

Gohl, K., Nitsche, F., & Miller, H. (1997). Seismic and gravity data reveal Tertiary interpolate subduction in the Bellingshausen Sea, southeast Pacific. *Geology*, *25*(4), 371–374. https://doi.org/10.1130/0091-7613(1997)025<0371:sagdrt>2.3.co;2

Gregori, D. A., Saini-Eidukat, B., Benedini, L., Strazzere, L., Barros, M., & Kostadinoff, J. (2016). The Gondwana orogeny in northern North Patagonian Massif: Evidence from the Caita Có granite, La Seña and Pangaré mylonites, Argentina. *Geoscience Frontiers*, *7*(4), 621–638. https://doi.org/10.1016/j.gsf.2015.06.002

Hervé, F., Faundez, V., Brix, M., & Fanning, C. M. (2006). Jurassic sedimentation of the Miers Bluff Formation, Livingston Island, Antarctica: Evidence from SHRIMP U-Pb ages of detrital and plutonic zircons. *Antarctic Science*, *18*(2), 229–238. https://doi.org/10.1017/s0954102006000277

Hervé, F., Lobato, J., Ugalde, I., & Pankhurst, R. J. (1996). The geology of Cape Dubouzet, northern Antarctic Peninsula: Continental basement to the Trinity Peninsula group? *Antarctic Science*, *8*(4), 407–414. https://doi.org/10.1017/s0954102096000582

Holdsworth, B. K., & Nell, P. A. R. (1992). Mesozoic radiolarian faunas from the Antarctic Peninsula: Age, tectonic and palaeoceanographic significance. *Journal of the Geological Society*, *149*(6), 1003–1020. https://doi.org/10.1144/gsjgs.149.6.1003

Hunter, M. A., & Cantrill, D. J. (2006). A new stratigraphy for the Latady basin, Antarctic Peninsula: Part 2, Latady group and basin evolution. *Geological Magazine*, *143*(6), 797–819. https://doi.org/10.1017/S0016756806002603

Hunter, M. A., Cantrill, D. J., Flowerdew, M. J., & Millar, I. L. (2005). Mid-jurassic age for the Botany Bay group: Implications for Weddell Sea basin creation and southern hemisphere biostratigraphy. *Journal of the Geological Society*, *162*(5), 745–748. https://doi.org/10.1144/0016-764905-051

Hunter, M. A., Riley, T. R., Cantrill, D. J., Flowerdew, M. J., & Millar, I. L. (2006). A new stratigraphy for the Latady basin, Antarctic Peninsula: Part 1, Ellsworth Land volcanic group. *Geological Magazine*, *143*(6), 777–796. https://doi.org/10.1017/s0016756806002597

Hyden, G., & Tanner, P. W. G. (1981). Late-Palaeozoic–early Mesozoic fore-arc basin sedimentary rocks at the Pacific margin in Western Antarctica. *Geologische Rundshau*, *70*(2), 529–541. https://doi.org/10.1007/bf01822133

Jeon, H., & Whitehouse, M. J. (2015). A critical evaluation of U–Pb calibration schemes used in SIMS zircon geochronology. *Geostandards and Geoanalytical Research*, *39*(4), 443–452. https://doi.org/10.1111/j.1751-908x.2014.00325.x

Jordan, T. A., Riley, T. R., & Siddoway, C. S. (2020). Anatomy and evolution of a complex continental margin: Geologic history of West Antarctica. *Nature Reviews Earth & Environment*, *1*(2), 117–133. https://doi.org/10.1038/s43017-019-0013-6

Kelly, S. R. A., Doubleday, P. A., Brunton, C. H. C., Dickins, J. M., Sevastopulo, G. D., & Taylor, P. D. (2001). First Carboniferous and? Permian marine macrofaunas from Antarctica and their tectonic implications. *Journal of the Geological Society*, *158*(2), 219–232. https://doi.org/10.1144/jgs.158.2.219

Larter, R. D., Cunningham, A. P., Barker, P. F., Gohl, K., & Nitsche, F. O. (2002). Tectonic evolution of the Pacific margin of Antarctica 1. Late Cretaceous tectonic reconstructions. *Journal of Geophysical Research*, *107*(B12), EPM5-1–EPM5-19. https://doi.org/10.1029/2000jb000052

Ludwig, K. R. (2012). *User manual for Isoplot 3.75-4.15: A geochronological toolkit for Microsoft excel* (Vol. 5). Berkeley Geochronology Centre Special Publications.

McCarron, J. J., & Larter, R. D. (1998). Late Cretaceous to early Tertiary subduction history of the Antarctic Peninsula. *Journal of the Geological Society*, *155*(2), 255–268. https://doi.org/10.1144/gsjgs.155.2.0255

McCarron, J. J., & Millar, I. L. (1997). The age and stratigraphy of fore-arc magmatism on Alexander Island, Antarctica. *Geological Magazine*, *134*(4), 507–522. https://doi.org/10.1017/s0016756897007437

Navarrete, C., Gianni, G., Encinas, A., Marquez, M., Kamerbeek, Y., Valle, M., & Folguera, A. (2019). Triassic to Middle Jurassic geodynamic evolution of southwestern Gondwana: From a large flat-slab to mantle plume suction in a rollback subduction setting. *Earth-Science Reviews*, *194*, 125–159. https://doi.org/10.1016/j.earscirev.2019.05.002

Nell, P. A. R. (1990). Deformation in an accretionary melange, Alexander Island, Antarctica. In J. Kniper & H. Ruttere (Eds.), *Deformation mechanisms, rheology and tectonics* (Vol. 54, pp. 405–416). Geological Society Special Publications.

Nelson, D. A., & Cottle, J. M. (2018). The secular development of accretionary orogens: Linking the Gondwana magmatic arc record of West Antarctica, Australia and South America. *Gondwana Research*, *63*, 15–33. https://doi.org/10.1016/J.GR.2018.06.002

Nelson, D. A., & Cottle, J. M. (2019). Tracking voluminous Permian volcanism of the Choiyoi province into central Antarctica. *Lithosphere*, *11*(3), 386–398. https://doi.org/10.1130/l1015.1

Pankhurst, R. J., Riley, T. R., Fanning, C. M., & Kelley, S. P. (2000). Episodic silicic volcanism in Patagonia and the Antarctic Peninsula: Chronology of magmatism associated with break-up of Gondwana. *Journal of Petrology*, *41*(5), 605–625. https://doi.org/10.1093/petrology/41.5.605

Riley, T. R., Burton-Johnson, A., Flowerdew, M. J., Poblete, F., Castillo, P., Hervé, F., et al. (2023). Palaeozoic—Early Mesozoic geological history of the Antarctic Peninsula and correlations to Patagonia: Kinematic reconstructions of the proto-Pacific margin of Gondwana. *Earth-Science Reviews*, *236*, 28. https://doi.org/10.1016/j.earscirev.2022.104265

Riley, T. R., Burton-Johnson, A., Flowerdew, M. J., & Whitehouse, M. J. (2018). Episodicity within a mid-Cretaceous magmatic flare-up in west Antarctica: U-Pb ages of the Lassiter coast intrusive suite, Antarctic Peninsula and correlations along the Gondwana margin. *The Geological Society of America Bulletin*, *130*(7–8), 1177–1196. https://doi.org/10.1130/B31800.1

Riley, T. R., Carter, A., Burton-Johnson, A., Leat, P. T., Hogan, K. A., & Bown, P. R. (2022). Crustal block origins of the South Scotia ridge. *Terra Nova*, *34*(6), 495–502. https://doi.org/10.1111/ter.12613

Riley, T. R., Flowerdew, M. J., Burton-Johnson, A., Leat, P. T., Millar, I. L., & Whitehouse, M. J. (2020). Cretaceous arc volcanism of Palmer Land, Antarctic Peninsula: Zircon U-Pb geochronology, geochemistry, distribution and field relationships. *Journal of Volcanology and Geothermal Research*, *401*, 106969. https://doi.org/10.1016/j.jvolgeores.2020.106969

Riley, T. R., Flowerdew, M. J., Millar, I. L., & Whitehouse, M. J. (2020). Triassic magmatism and metamorphism in the Antarctic Peninsula: Identifying the extent and timing of the Gondwanide orogeny. *Journal of South American Earth Sciences*, *103*, 102732. https://doi.org/10.1016/j.jsames.2020.102732

Riley, T. R., Flowerdew, M. J., Pankhurst, R. J., Leat, P. T., Millar, I. L., Fanning, C. M., & Whitehouse, M. J. (2017). A revised geochronology of Thurston Island, West Antarctica and correlations along the proto-Pacific margin of Gondwana. *Antarctic Science*, *29*(1), 47–60. https://doi.org/10.1017/s0954102016000341

Riley, T. R., Flowerdew, M. J., Pankhurst, R. J., Millar, I. L., & Whitehouse, M. J. (2020). Late Mesoproterozoic magmatism and metamorphism of Haag Nunataks, Coats Land and Shackleton Range (Antarctica); new U-Pb zircon geochronology constraining the extent of juvenile arc terranes. *Precambrian Research*, *340*, 105646. https://doi.org/10.1016/j.precamres.2020.105646

Robertson, A. H. F., Campbell, H. C., Johnston, M., & Mortimer, N. (2019). Introduction to Palaeozoic–Mesozoic geology of south island, New Zealand: Subduction-related processes adjacent to SE Gondwana. In A. H. F. Robertson (Ed.), *Palaeozoic–Mesozoic geology of South island, New Zealand: Subduction-related processes adjacent to SE Gondwana* (Vol. 49, pp. 1–14). Geological Society.

Sepúlveda, F. A., Palma-Heldt, S., Hervé, F., & Fanning, C. M. (2010). Permian depositional age of metaturbidites of the Duque de York complex, southern Chile: U-Pb SHRIMP data and palynology. *Andean Geology*, *37*, 275–397.

Simões Pereira, P., van de Flierdt, T., Hemming, S. R., Hammond, S. J., Kuhn, G., Brachfeld, S., et al. (2018). Geochemical fingerprints of glacially eroded bedrock from West Antarctica: Detrital thermochronology, radiogenic isotope systematics and trace element geochemistry in Late Holocene glacial-marine sediments. *Earth-Science Reviews*, *182*, 204–232. https://doi.org/10.1016/j.earscirev.2018.04.011

Sláma, J., Košler, J., Condon, D. J., Crowley, J. L., Gerdes, A., Hanchar, J. M., et al. (2008). Plešovice zircon—A new natural reference material for U–Pb and Hf isotopic microanalysis. *Chemical Geology*, *249*(1–2), 1–35. https://doi.org/10.1016/j.chemgeo.2007.11.005

Smellie, J. L., & Hole, M. J. (2021). Antarctic Peninsula: Volcanology. In J. L. Smellie, et al. (Eds.), *Volcanism in Antarctica: 200 million years of subduction, rifting and continental break-up* (Vol. 55, pp. 305–325). Geology Society London Memoir.

Söderlund, U., Patchett, P. J., Vervoort, J. D., & Isachsen, C. E. (2004). The ^{176}Lu decay constant determined by Lu-Hf and U–Pb isotope systematics of Precambrian mafic intrusions. *Earth and Planetary Science Letters*, *219*(3), 311–324. https://doi.org/10.1016/s0012-821x(04)00012-3

Stacey, J. S., & Kramers, J. D. (1975). Approximation of terrestrial lead evolution by a two-stage model. *Earth and Planetary Science Letters*, *26*(2), 207–221. https://doi.org/10.1016/0012-821x(75)90088-6

Storey, B. C., Thomson, M. R. A., & Meneilly, A. W. (1987). The Gondwanian orogeny within the Antarctic Peninsula: A discussion. In G. D. McKenzie (Ed.), *Gondwana six: Structure, tectonics and geophysics* (Vol. 40, pp. 191–198). Geophysical Monograph.

Storey, B. C., Vaughan, A. P. M., & Millar, I. L. (1996). Geodynamic evolution of the Antarctic Peninsula during Mesozoic times and its bearing on Weddell Sea history. *Geological Society of London, Special Publication*, *108*(1), 87–103. https://doi.org/10.1144/gsl.sp.1996.108.01.07

Suárez, M. (1976). Plate tectonic model for southern Antarctic Peninsula and its relation to southern Andes. *Geology*, *4*, 211–214. https://doi.org/10.1130/0091-7613(1976)4<211:pmfsap>2.0.co;2

Thomson, M. R. A. (1975). New palaeontological and lithological observations on the Legoupil Formation, northwest Antarctic Peninsula. *British Antarctic Survey Bulletin*, *41/42*, 169–185.

Thomson, M. R. A., & Pankhurst, R. J. (1983). Age of post-Gonwanian calc-alkaline volcanism in the Antarctic Peninsula region. In R. L. Oliver, et al. (Eds.), *Antarctic Earth science* (pp. 328–333). Australian Academy of Science.

Thomson, M. R. A., & Tranter, T. H. (1986). Early jurassic fossils from central Alexander island and their geological setting: British Antarctic Survey. *Bulletin*, *70*, 23–39.

Tranter, T. H. (1987). The structural history of the LeMay group of central Alexander island, Antarctic Peninsula. *British Antarctic Survey Bulletin*, *77*, 61–80.

Tranter, T. H. (1988). *The tectonostratigraphic history of the LeMay Group if central Alexander island, Antarctica*. Ph.D. Thesis (p. 272). Council for National Academic Awards.

Tranter, T. H. (1991). Accretion and subduction processes along the Pacific margin of Gondwana, central Alexander Island, In M. R. A. Thomson, et al. (Eds.). In *Geological evolution of Antarctica* (pp. 437–441). Cambridge University Press.

Trouw, R. A. J., Passchier, C. W., Simoes, L. S. A., Andreis, R. R., & Valeriano, C. M. (1997). Mesozoic tectonic evolution of the South Orkney microcontinent, Scotia arc, Antarctica. *Geological Magazine*, *134*(3), 383–401. https://doi.org/10.1017/s0016756897007036

Trouw, R. A. J., Simoes, L. S. A., & Valladares, C. (1998). Metamorphic evolution of a subduction complex, South Shetland islands, Antarctica. *Journal of Metamorphic Geology*, *16*(4), 475–490. https://doi.org/10.1111/j.1525-1314.1998.00151.x

Twinn, G., Riley, T. R., Fox, M., & Carter, A. (2022). Thermal history of the southern Antarctic Peninsula during Cenozoic oblique subduction. *Journal of the Geological Society*, *176*(6). https://doi.org/10.1144/jgs2022-008

Umhoefer, P. J., & Dorsey, R. J. (1997). Translation of terranes: Lessons from central baja California, Mexico. *Geology*, *25*(11), 1007–1010. https://doi.org/10.1130/0091-7613(1997)025<1007:totlfc>2.3.co;2

Vaughan, A. P. M., Eagles, G., & Flowerdew, M. J. (2012). Evidence for a two-phase Palmer Land event from crosscutting structural relationships and emplacement timing of the Lassiter coast intrusive suite, Antarctic Peninsula: Implications for mid-Cretaceous southern ocean plate configuration. *Tectonics*, *31*(1), 1010. https://doi.org/10.1029/2011tc003006

Vaughan, A. P. M., Pankhurst, R. J., & Fanning, C. M. (2002). A mid-Cretaceous age for the Palmer Land event: Implications for terrane accretion timing and Gondwana palaeolatitudes. *Journal of the Geological Society*, *159*(2), 113–116. https://doi.org/10.1144/0016-764901-090

Vaughan, A. P. M., & Storey, B. C. (2000). The eastern Palmer Land shear zone: A new terrane accretion model for the Mesozoic development of the Antarctic Peninsula. *Journal of the Geological Society*, *157*(6), 1243–1256. https://doi.org/10.1144/jgs.157.6.1243

Vermeesch, P. (2018). IsoplotR: A free and open toolbox for geochronology. *Geoscience Frontiers*, *9*(5), 1479–1493. https://doi.org/10.1016/j.gsf.2018.04.001

Vermeesch, P. (2021). Maximum depositional age estimation revisited. *Geoscience Frontiers*, *12*(2), 843–850. https://doi.org/10.1016/j.gsf.2020.08.008

Vermeesch, P., Resentini, A., & Garzanti, E. (2016). An R package for statistical provenance analysis. *Sedimentary Geology*, *336*, 14–25. https://doi.org/10.1016/j.sedgeo.2016.01.009

Wendt, A. S., Vaughan, A. P. M., & Tate, A. J. (2008). Metamorphic rocks in the Antarctic Peninsula region. *Geological Magazine*, *145*(5), 655–676. https://doi.org/10.1017/S0016756808005050

Whitehouse, M. J., & Kamber, B. S. (2005). Assigning dates to thin gneissic veins in high-grade metamorphic terranes: A cautionary tale from Akilia, southwest Greenland. *Journal of Petrology*, *46*(2), 291–318. https://doi.org/10.1093/petrology/egh075

Willan, R. C. R. (2003). Provenance of Triassic – Cretaceous sandstones in the Antarctic Peninsula: Implications for terrane models during Gondwana breakup. *Journal of Sedimentary Research*, *73*(6), 1062–1077. https://doi.org/10.1306/050103731062

Willner, A. P., Sepúlveda, F. A., Herve, F., Massone, H. J., & Sudo, F. (2009). Conditions and timing of Pumpellyite-Actinolite-facies metamorphism in the early Mesozoic frontal accretionary prism of the Madre de Dios Archipelago (Latitude 50°20′S; southern Chile). *Journal of Petrology*, *50*(11), 2127–2155. https://doi.org/10.1093/petrology/egp071

References From the Supporting Information

Adams, C. J., Campbell, H. J., & Griffin, W. R. (2007). Provenance comparisons of Permian to Jurassic tectonostratigraphic terranes in New Zealand: Perspectives from detrital zircon age patterns. *Geological Magazine*, *144*(4), 701–729. https://doi.org/10.1017/s0016756807003469

Barbeau, D. L., Jr., Gombosi, D. J., Zahid, K. M., Bizimis, M., Swanson-Hysell, N., Valencia, V., & Gehrels, G. E. (2009). U-Pb zircon constraints on the age and provenance of the Rocas Verdes basin fill, Tierra del Fuego, Argentina. *Geochemistry, Geophysics, Geosystems*, *10*(12), Q12001. https://doi.org/10.1029/2009gc002749

Bea, F., Montero, B., Molina, J. F., Scarrow, J. H., Cambeses, A., & Moreno, J. A. (2018). Lu-Hf ratios of crustal rocks and their bearing on zircon Hf isotope model ages: The effects of accessories. *Chemical Geology*, *484*, 179–190. https://doi.org/10.1016/j.chemgeo.2017.11.034

Corfu, F., & Ayres, L. D. (1984). U-Pb age and genetic significance of heterogeneous zircon populations in rocks from the Favourable Lake area, Northwestern Ontario. *Contributions to Mineralogy and Petrology*, *88*(1), 86–101. https://doi.org/10.1007/bf00371414

Corfu, F., & Noble, S. (1992). Genesis of the southern Abitibi greenstone belt, Superior Province, Canada: Evidence from zircon Hf-isotope analysis using a single filament technique. *Geochimica et Cosmochima Acta*, *56*(5), 2081–2097. https://doi.org/10.1016/0016-7037(92)90331-c

Elliot, D. H., Fanning, C. M., Mukasa, S. B., & Millar, I. L. (2019). Hf- and O-isotope data from detrital and granitoid zircons reveal characteristics of the Permian-Triassic magmatic belt along the Antarctic sector of Gondwana. *Geosphere*, *15*(2), 576–604. https://doi.org/10.1130/ges02011.1

Krogh, T. E., & Davis, G. L. (1985). *The production and preparation of ^{205}Pb for use as a tracer for isotope dilution analysis* (Vol. 74, pp. 416–417). Year Book Carnegie Institute.

Ludwig, K. R. (1989). *PBDAT: A computer program for processing Pb-U-Th isotope data, version 1.20* (pp. 88–542). U.S. Geological Survey Open File Report.

Nasdala, L., Hofmeister, W., Norberg, N., Mattinson, J.M., Corfu, F., Dörr, W., et al. (2008). Zircon M257 – A homogeneous natural reference material for the ion microprobe U-Pb analysis of zircon. *Geostandards and Geoanalytical Research*, *32*(3), 247–265. https://doi.org/10.1111/j.1751-908x.2008.00914.x

Nowell, G.M., & Parrish, R.R. (2001). Simultaneous acquisition of isotope compositions and parent/daughter ratios by non-isotope dilution-mode plasma ionisation multi-collector mass spectrometry (PIMMS). In G. Holland & S.D. Tanner (Eds.), *Plasma Source Mass Spectrometry: The New Millenium* (Vol. 267, pp. 298–310). Royal Soc. Chem., Spec. Publ.

Paces, J. B., & Miller, J. D. (1993013). Precise U-Pb ages of Duluth Complex and related mafic intrusions, northeastern Minnesota: Geochronological insights to physical, petrogenetic, paleomagnetic, and tectonomagmatic process associated with the 1.1 Ga Midcontinent Rift System. *Journal of Geophysical Research-Solid Earth*, *98B*(13), 13997–14013. https://doi.org/10.1029/93JB01159

Paton, C., Hellstrom, J., Paul, B., Woodhead, J., & Hergt, J. (2011). Iolite: Freeware for the visualisation and processing of mass spectrometric data. *Journal of Analytical Atomic Spectrometry*, *26*(12), 2508. https://doi.org/10.1039/c1ja10172k

Pointon, M. A., Cliff, R. A., & Chew, D. (2012). The provenance of Western Irish Namurian Basin sedimentary strata inferred using detrital zircon U–Pb LA-ICP-MS geochronology. *Geological Journal*, *47*(1), 77–98. https://doi.org/10.1002/gj.1335

Renne, P. R., Swisher, C. C., ADeino, A. L., Karner, D. B., Owens, T. L., & DePaolo, D. J. (1998). Intercalibration of standards, absolute ages and uncertainties in ^{40}Ar/^{39}Ar dating. *Chemical Geology*, *145*(1–2), 117–152. https://doi.org/10.1016/s0009-2541(97)00159-9

Riley, T. R., Carter, A., Burton-Johnson, A., Leat, P. T., Hogan, K. A., & Bown, P. R. (2022). Crustal block origins of the South Scotia Ridge. *Terra Nova*, *34*(6), 495–502. https://doi.org/10.1111/ter.12613

Steiger, R. H., & Jager, E. (1977). Subcommission on geochronology: Convention on the use of decay constants in geo- and cosmochronology. *Earth and Planetary Science Letters*, *36*(3), 359–362. https://doi.org/10.1016/0012-821x(77)90060-7

Wiedenbeck, M., Alle, P., Corfu, F., Griffin, W. L., Meirer, M., Oberli, F., et al. (1995). Three natural zircon standards for U-Th-Pb, Lu-Hf, trace element and REE analyses. *Geostandards Newsletter*, *19*, 1–23. https://doi.org/10.1111/j.1751-908x.1995.tb00147.x

Woodhead, J. D., & Hergt, J. M. (2005). A preliminary appraisal of seven natural zircon reference materials for in situ Hf isotope determination. *Geostandards and Geoanalytical Research*, *29*(2), 183–195. https://doi.org/10.1111/j.1751-908x.2005.tb00891.x